Dust and structure in GCC fields

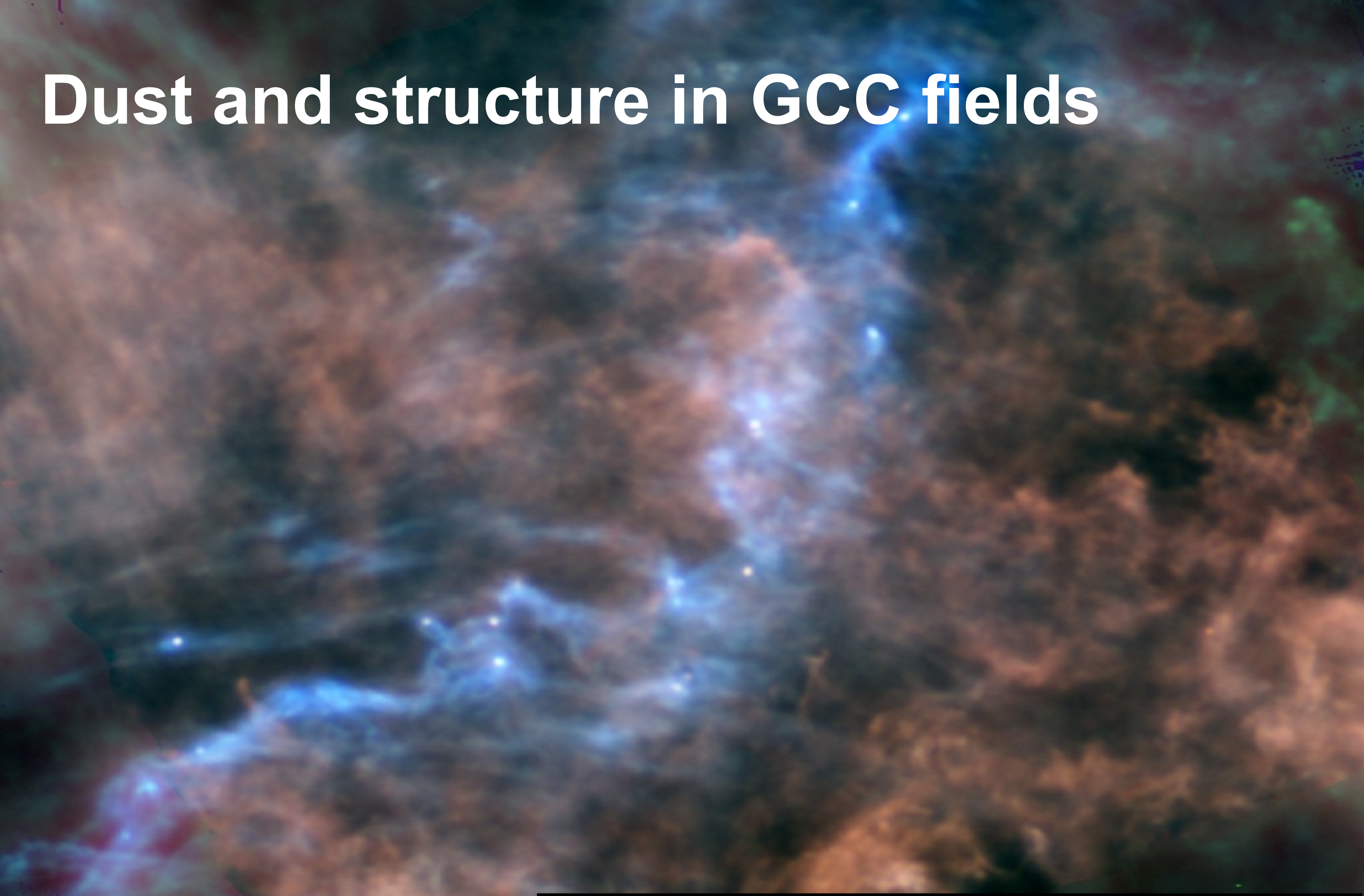

Galactic Cold Cores

M.Juvela University of Helsinki

How do stars form?

The formation of a star takes millions of years and results from a complex interplay of **gravitation**, **turbulence**, **thermal pressure**, **magnetic forces**, and **external triggering** (e.g. supernovae).

To **understand** this process, we need to study many sources at different stages of evolution.

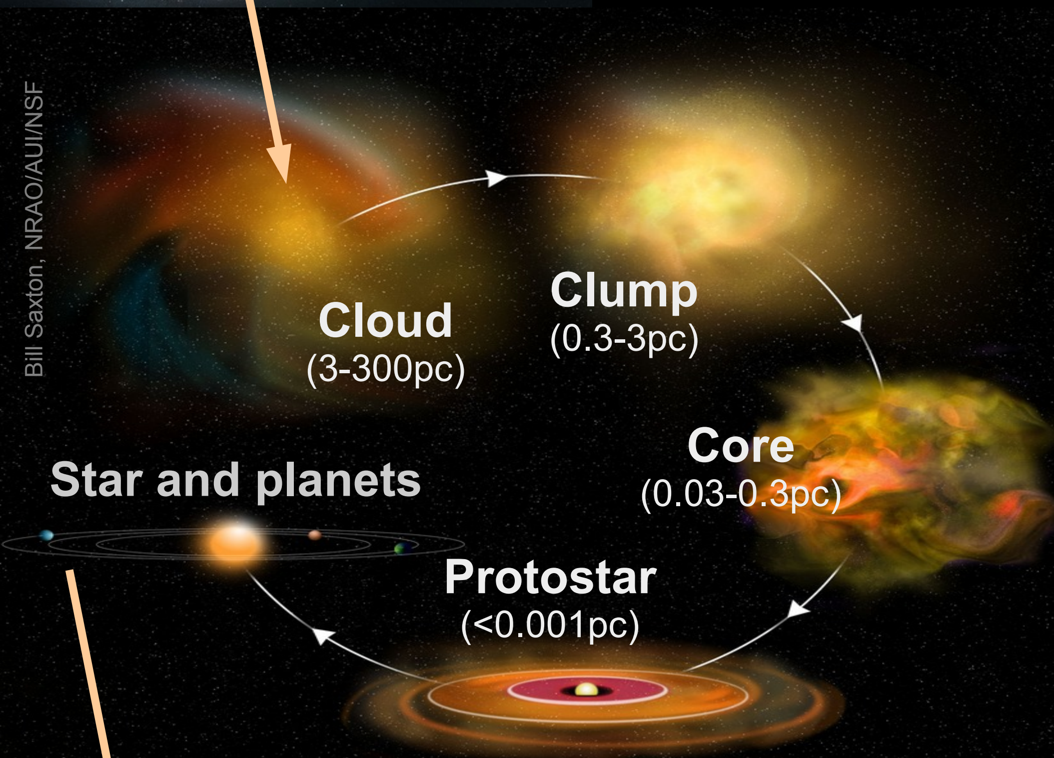

Structure of interstellar medium (ISM) is mapped with **observations of dust** (extinction, emission, scattering) **and gas** (radio emission lines), using the best instruments in the world.

Numerical **modelling** is developed and used to study clouds, clumps, and cores **as systems** with couplings between dynamics (MHD), radiative transfer, chemistry, dust properties, magnetic fields, and the heating and cooling processes.

Chemistry and dust properties trace cloud evolution. For example, the growth of dust particles is a continuous process from diffuse clouds to planets.

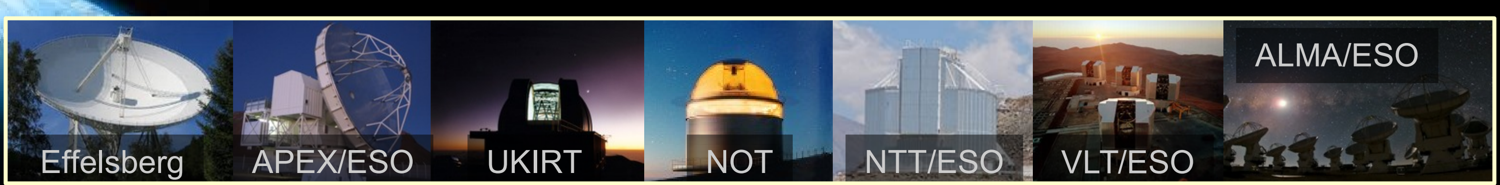

Planck (350μm – 1cm) from diffuse medium to dense clouds and clumps

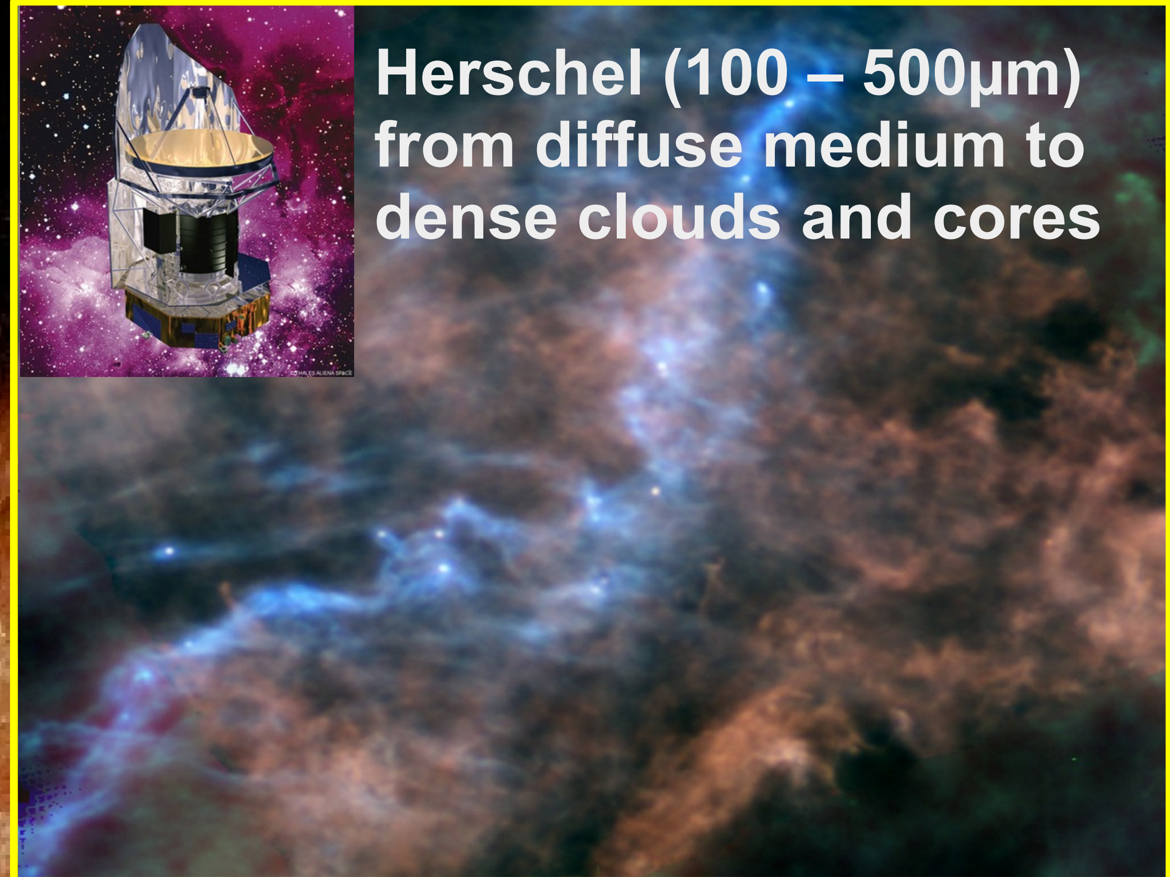

Herschel (100 – 500μm) from diffuse medium to dense clouds and cores

- Planck project **Cold Cores**
  - coordinators **I. Ristorcelli** and M. Juvela
- Herschel key programme **Galactic Cold Cores**
  - PI **M. Juvela**

Other projects following from the Planck survey:
Spitzer programme **Hunting coreshine** (R. Paladini)
ESO public survey in molecular line (Ke Wang)
JCMT/SCUBA-II legacy survey in continuum (Liu Tie)

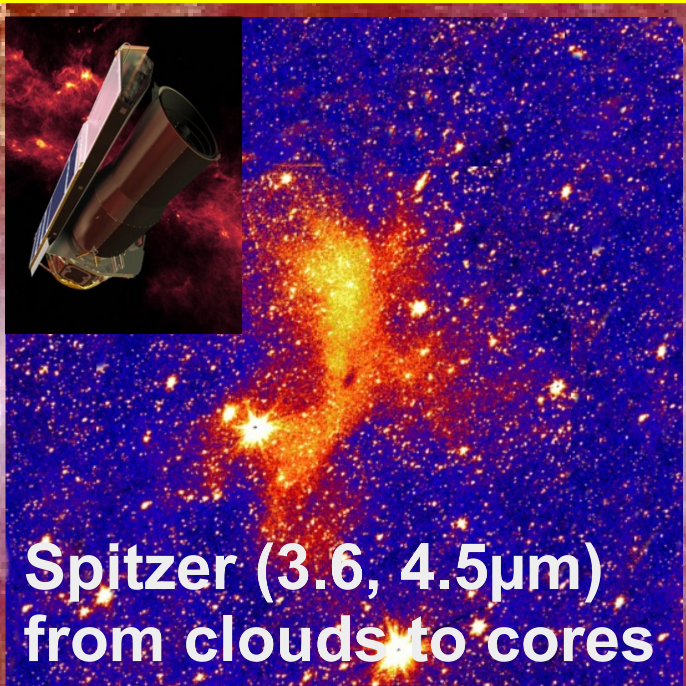

Spitzer (3.6, 4.5μm) from clouds to cores

PGCC: Planck catalogue of Galactic Cold **Clumps**

- released Jan 2015
- Over 13 000 sources
- Distances from 100pc to 8kpc, Galactic heights up to ± 400pc

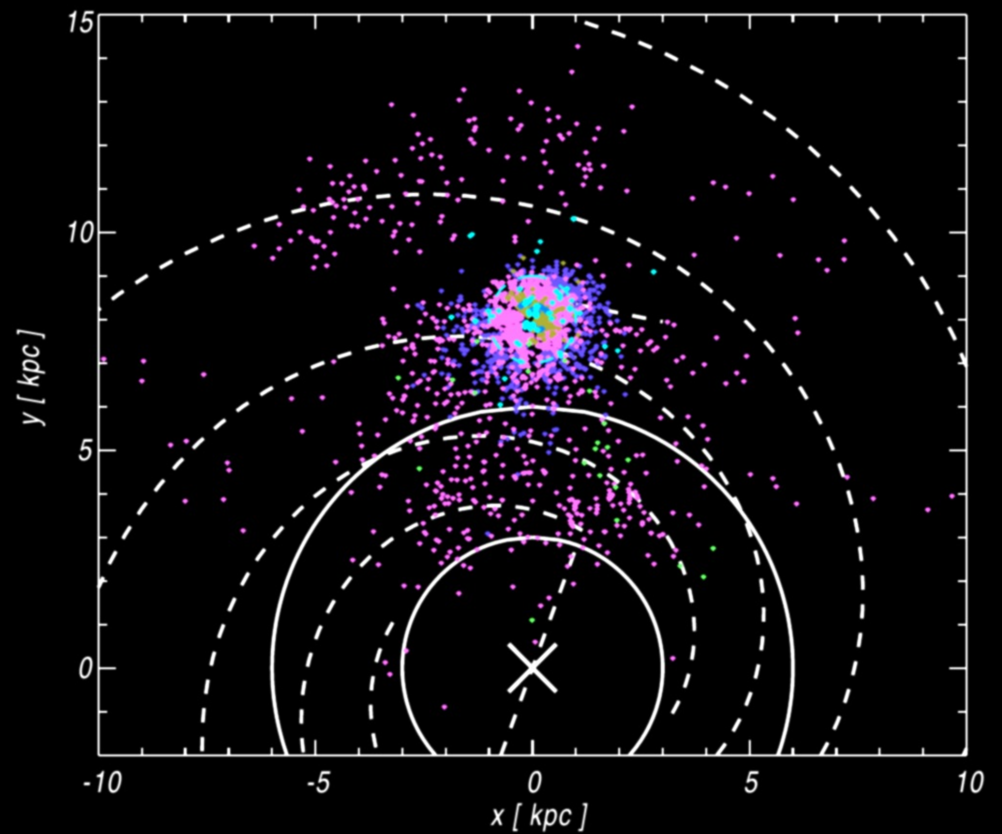

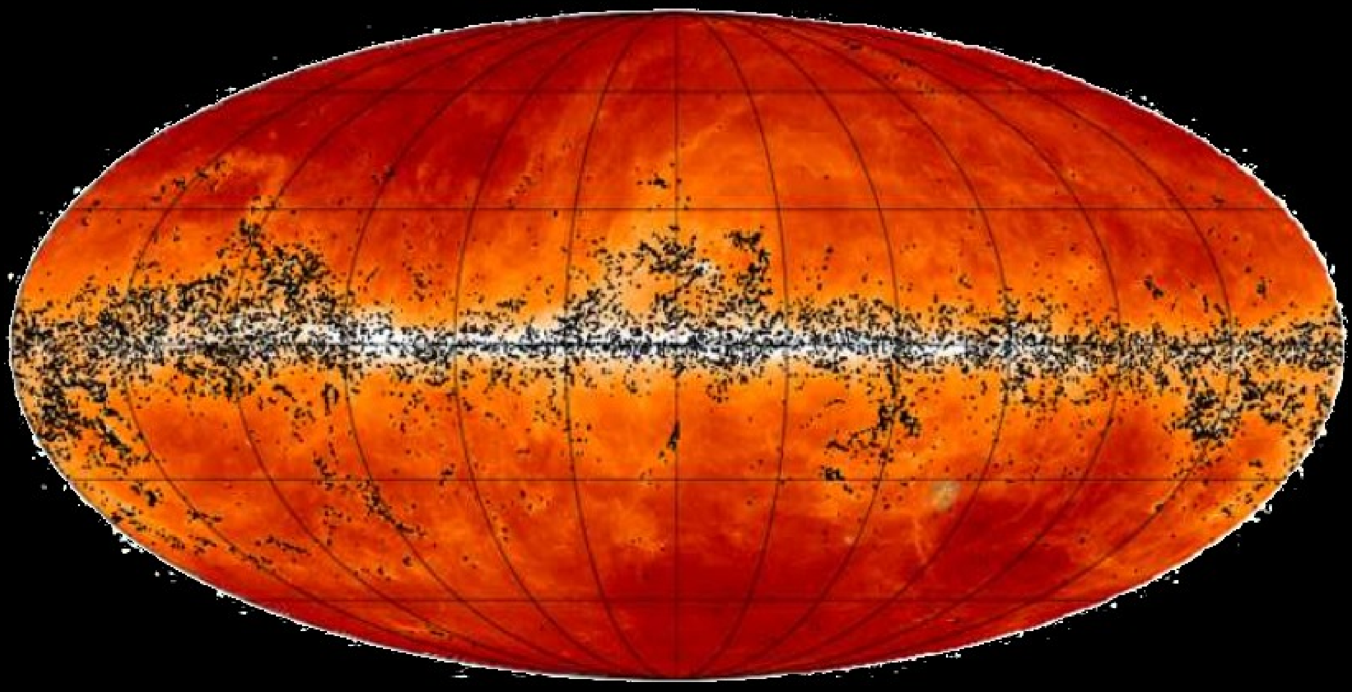

Planck Collaboration

Planck early results XXIII, A&A 536, A23 (2011)

Planck 2015 results. XXVIII: The Planck Catalogue of Galactic Cold Clumps

PGCC follow-up with Herschel

Galactic Cold Cores

- Herschel open time key programme (151h)
- 116 fields, ~40' in size, covering ~400 PGCC sources
- a **cross-section** of the full source population (*T*, *M*, *n*, *R*, *l*, *b* etc.)

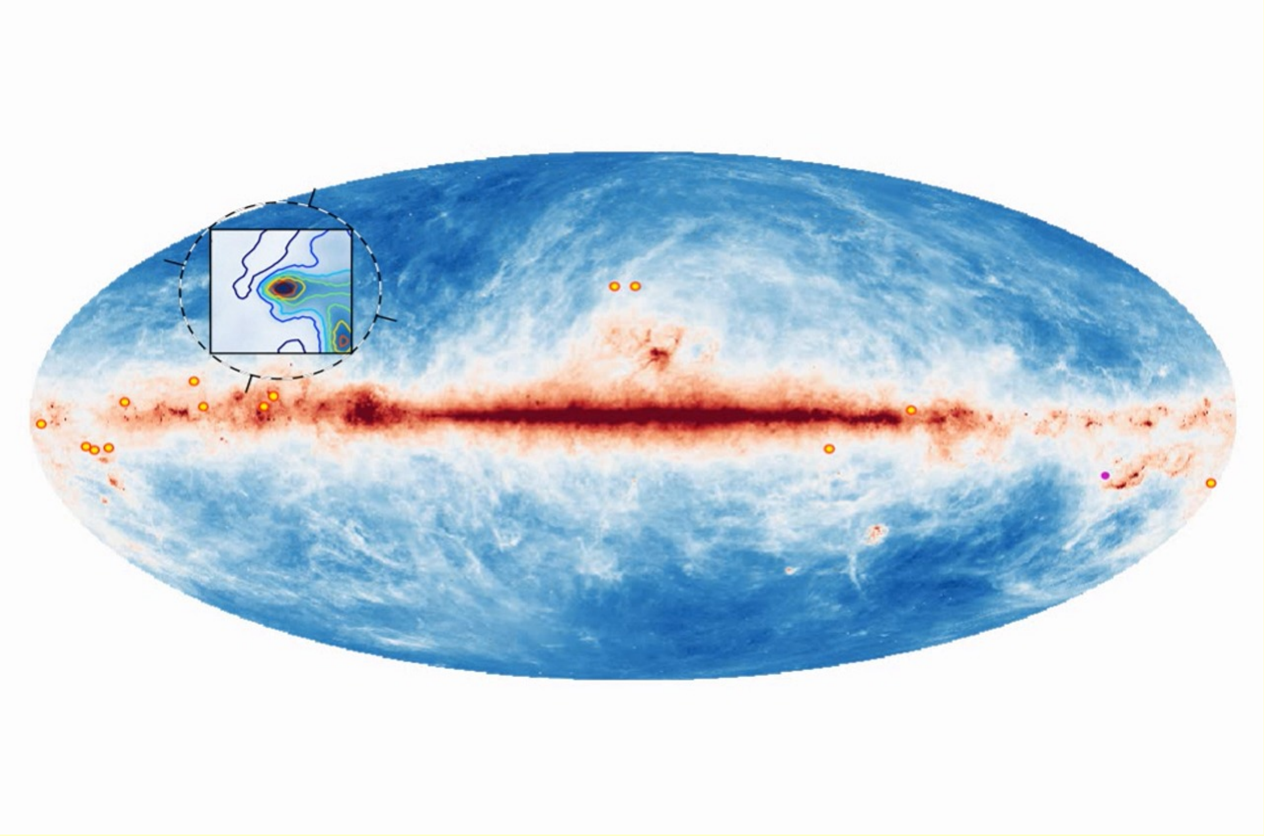

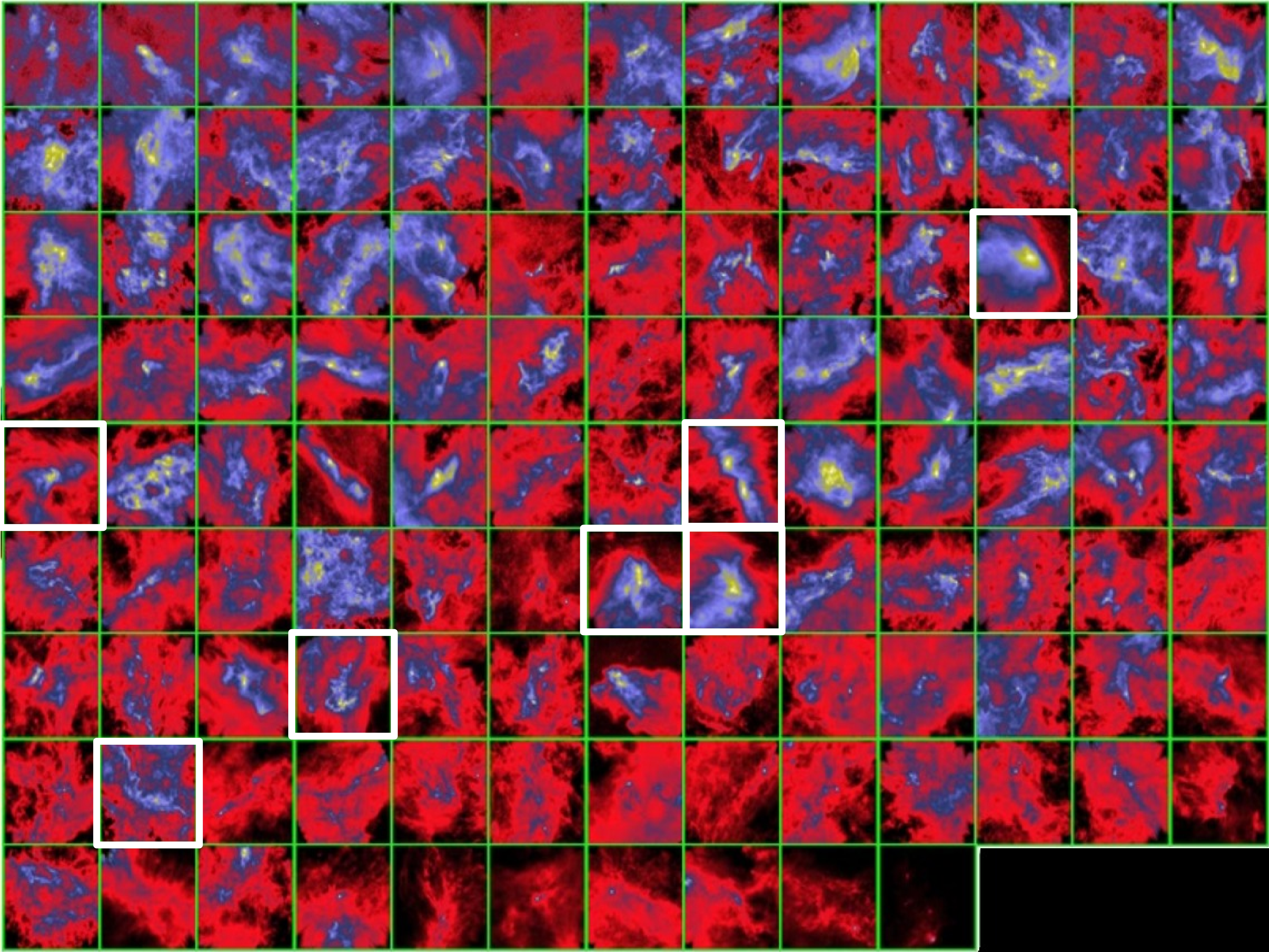

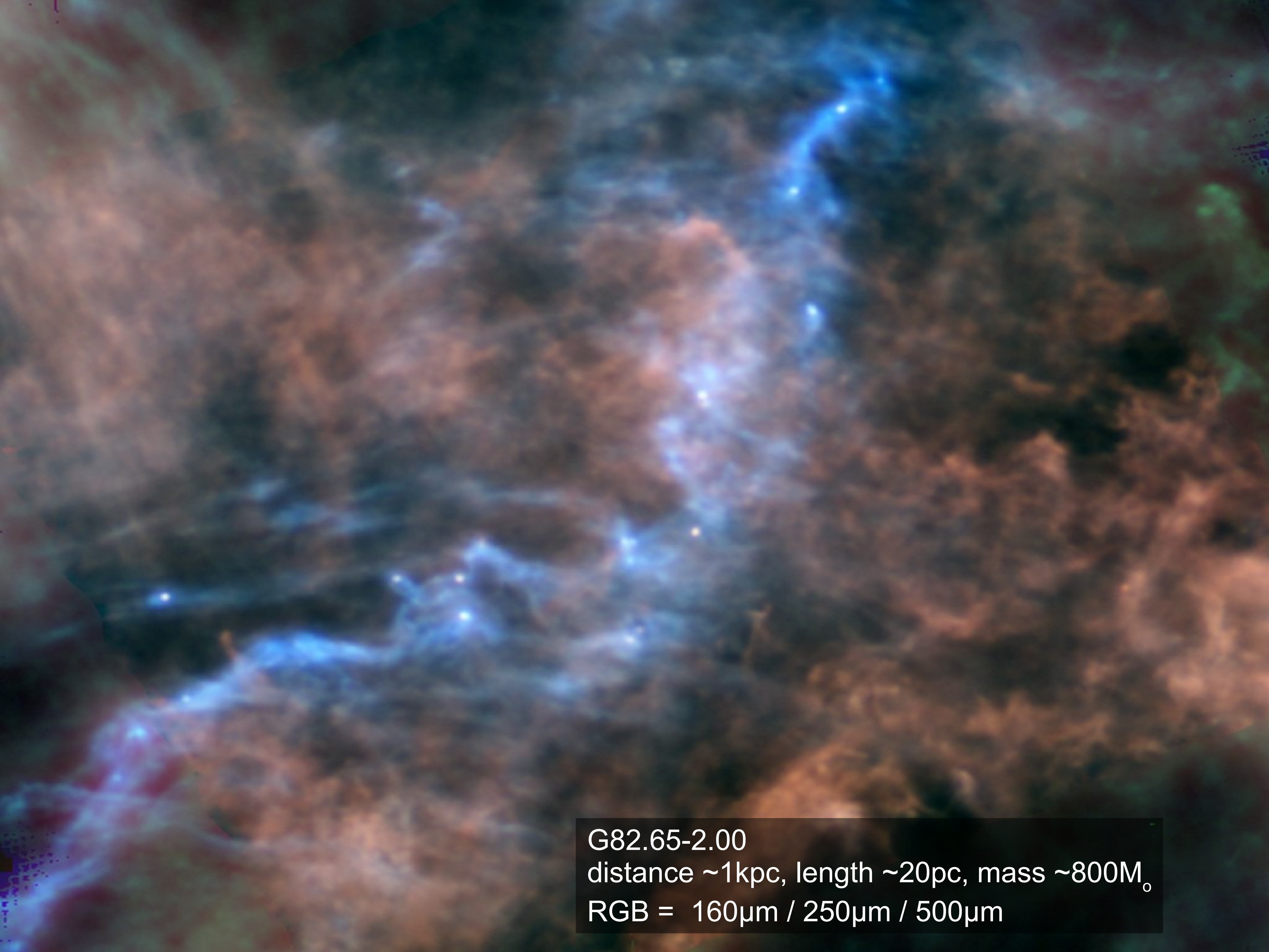
G82.65-2.00
distance ~1kpc, length ~20pc, mass ~800M_o
RGB = 160μm / 250μm / 500μm

Galactic Cold Cores. IV:
Clumps, star formation

Galactic Cold Cores. V:
Dust Opacity

Galactic Cold Cores. VI:
Dust spectral index

Juvela & Ysard 2012: *The effect of temperature mixing on the observable (T, β) -relation...*; **Juvela & Ysard** 2012: *The degeneracy between the dust colour temperature and the spectral index;* **Malinen, Juvela, Collins, Lunttila, Padoan** P 2011: *Accuracy of core mass estimates in simulated observations of dust emission*; **Ysard, Juvela** et al. 2012: Modelling the dust emission from dense interstellar clouds; ...

Galactic Cold Cores. VII-VIII:
Filaments *accepted/submitted*

Juvela et al. 2011: *Galactic cold cores II*; **Juvela, Malinen, Lunttila**, 2012: *The profile of interstellar cloud filaments: Observational ...*; **Malinen, Juvela, Rawlings** 2012: *Profiling filaments: comparing NIR extinction and sub-millimetre data...*; **Juvela** et al. 2012: *Profiles of interstellar cloud filaments: Observational effects in...*

Galactic Cold Cores. IX:
High latitude clouds *in prep.*

Malinen, Juvela, Zahorecz et al. 2014: *Multiwavelength study of the high-latitude cloud L1642: chain of star formation*; **Malinen** et al. 2016: *Dust polarisation...*

Galactic Cold Cores X:
Clump structure *in prep.*

Juvela, Malinen, Lunttila 2012: *Estimation of high-resolution dust column density maps. Comparison of …*; **Lunttila & Juvela** 2012: *Radiative transfer on hierarchial grids*; **Juvela & Montillaud** 2013: *Estimation of high-resolution dust column density maps. Empirical model …*

Dust Opacity

- what is the value of dust opacity
    - in practice, the ratio of submillimetre and near-infrared optical depths **$\tau(250\mu m) / \tau(J)$**
  - how does it differ from values in diffuse clouds
  - how does it vary between regions
  - how does it vary within a field

Galactic cold cores V. Dust opacity ⋆ ⋆⋆

M. Juvela[1], I. Ristorcelli[2,3], D.J. Marshall[4], J. Montillaud[1,5], V.-M. Pelkonen[1,6], N. Ysard[7], P. McGehee[8], R. Paladini[8], L. Pagani[9], J. Malinen[1], A. Rivera-Ingraham[2], C. Lefèvre[9] L.V. Tóth[10], L.A. Montier[2,3], J.-P. Bernard[2,3], P. Martin

$$\tau(250\mu m) = \frac{I_\nu(250\mu m)}{B_\nu(T)}$$

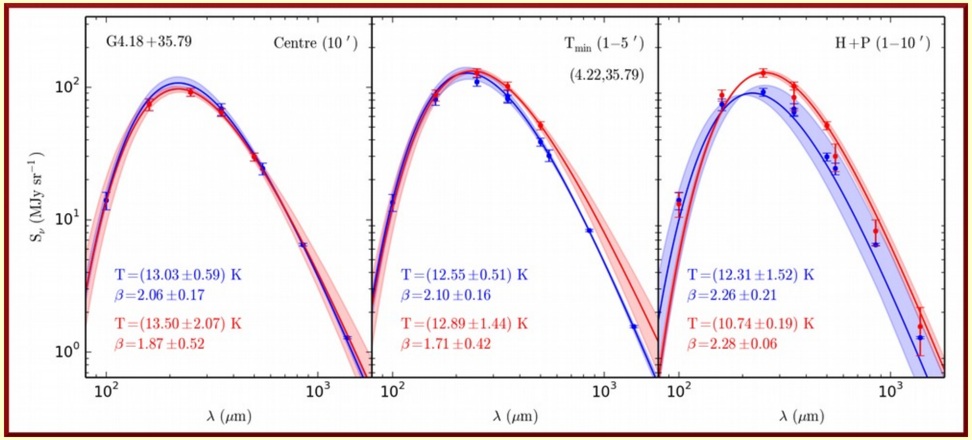

Dust optical depth τ(250μm)

- modified black body fits 100-500μm, 250-500μm
  - SPIRE provides larger area, more reliable data
  - shorter wavelengths (PACS) give better constraints of temperature; biased towards warmer dust
  - spectral index **fixed** to a value of **β=2.0**
    - higher than values ~1.8 found in diffuse medium
    - could be representative of dense clumps
    - ~30% effect on absolute (and relative) κ values

Near-infrared optical depth τ_J

- using the reddening of the background stars
  - **NICER**: combining J-H and H-K colour excesses
    - 2MASS survey: J, H, K bands (1.25-2.2μm)
    - a few fields covered by VISTA surveys
  - limited by the **number of stars**: 2'-3' resolution for nearby fields, nothing for the most distant ones!
  - depends on the shape of the extinction curve, which is relatively constant

Bias in τ(250μm)

$$\tau(250\mu m) = \frac{I_\nu(250\mu m)}{B_\nu(T)}$$

- line-of-sight temperature variations
  → colour temperature > mass-averaged *T*
  → τ underestimated
- corrections based on modelling
  - 3D cloud model matched to observations, Gaussian density profile along the line-of-sight
  - analyse synthetic maps, compare to the model column density → **estimated fractional correction**
- uncertainties
  - radiation field anisotropy
  - line-of-sight density structure
  - ratio between submm and optical dust opacity

Musca filament

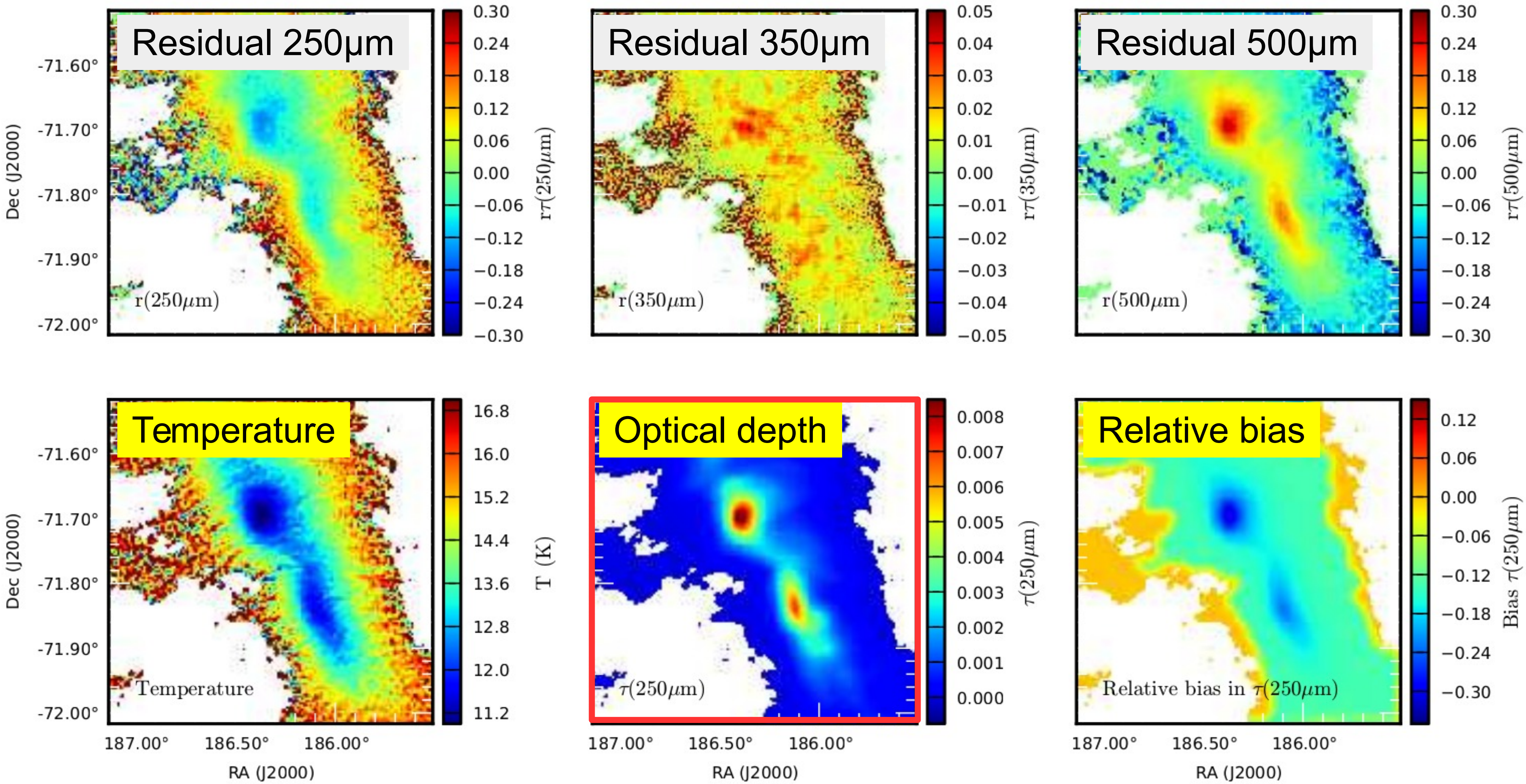

Upper row: residuals in fits to three SPIRE bands

Lower row: model T_C, optical depth, **relative bias**

Bias in $\tau(J)$

- *two* problems
  - **stellar density** decreases with column density
    → τ biased towards lower values
    - depends more on gradients than absolute value of extinction
  - distant fields contamination by **foreground stars**
- correction again based on simulations
  - τ map from Hershel data (18") → simulate different realisations of background stars
  - number of foreground stars deduced based on **Besancon** model
  - other statistics (intrinsic stellar colours etc.) derived from a reference region
  - comparison of inputs and outputs
    → **estimated fractional corrections**

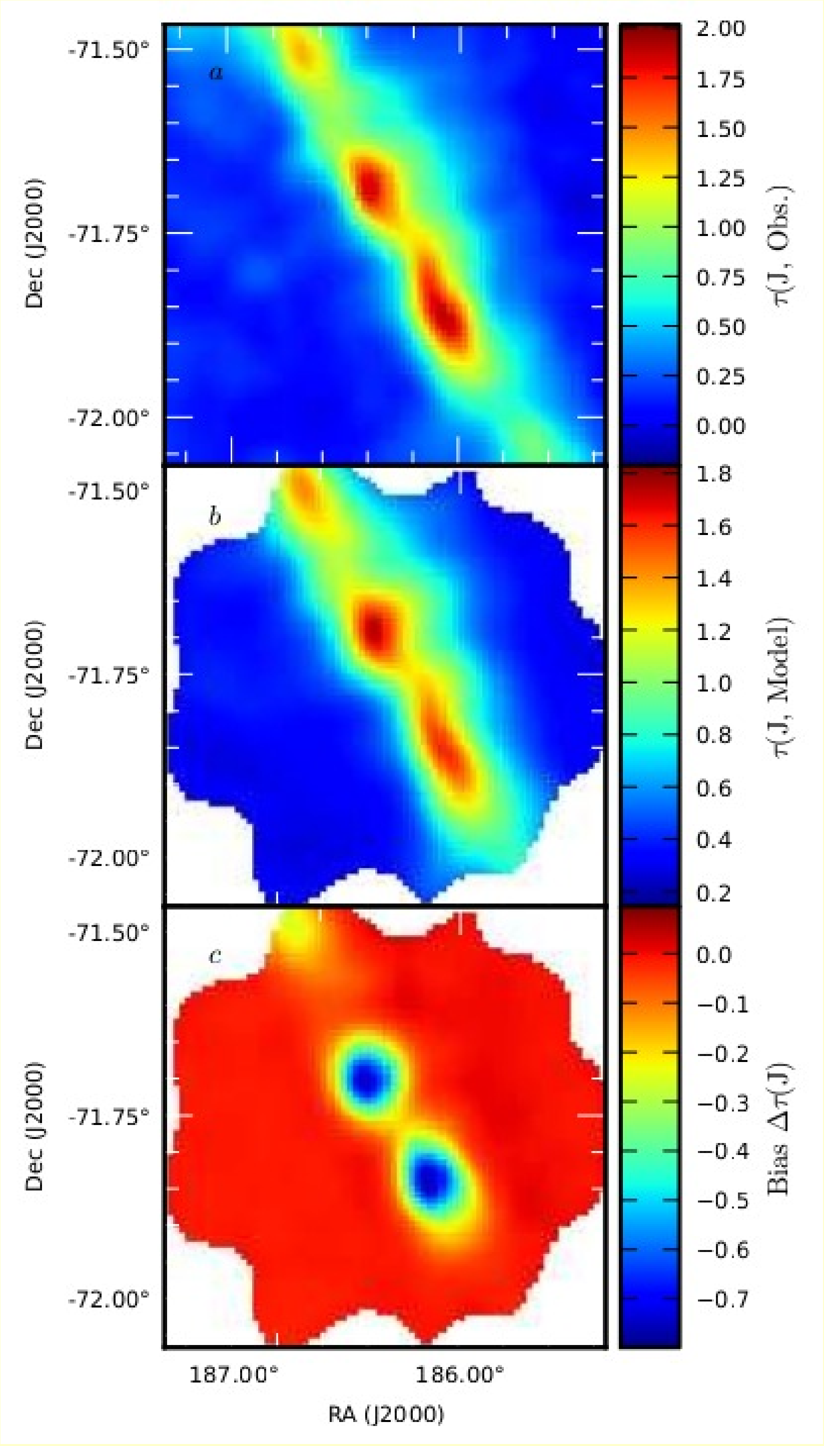

Model of NIR **optical depth** (from Herschel)

Simulated **NICER map** (average of 100 realisations)

Estimate of absolute **bias =** <simulations> - input τ

Based on the uncertainty of *k*, only the **21 most reliable** **selected** out of the original sample of 116 fields

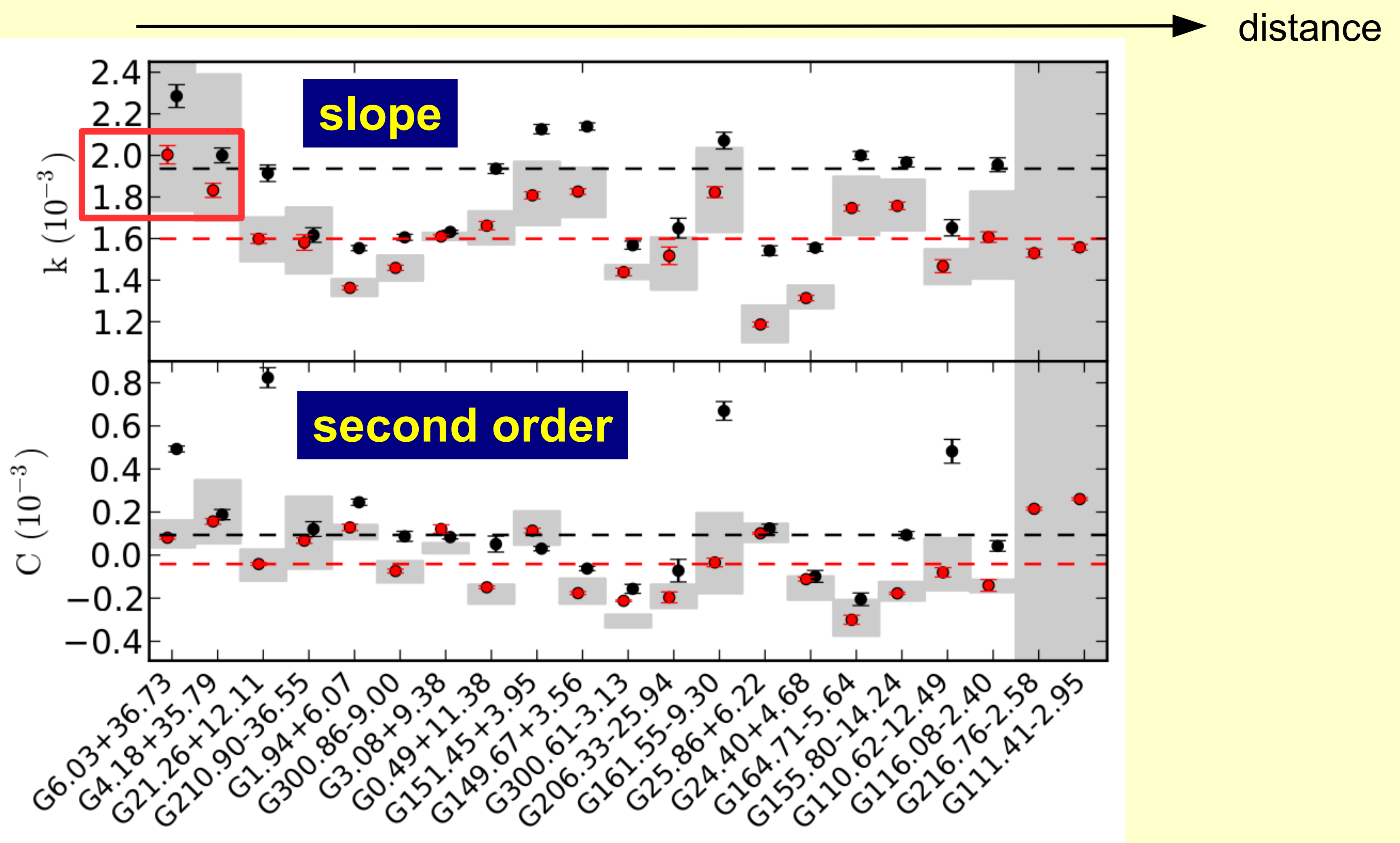

Gray bands = uncertainty of the distance !

Before bias corrections **After** the corrections

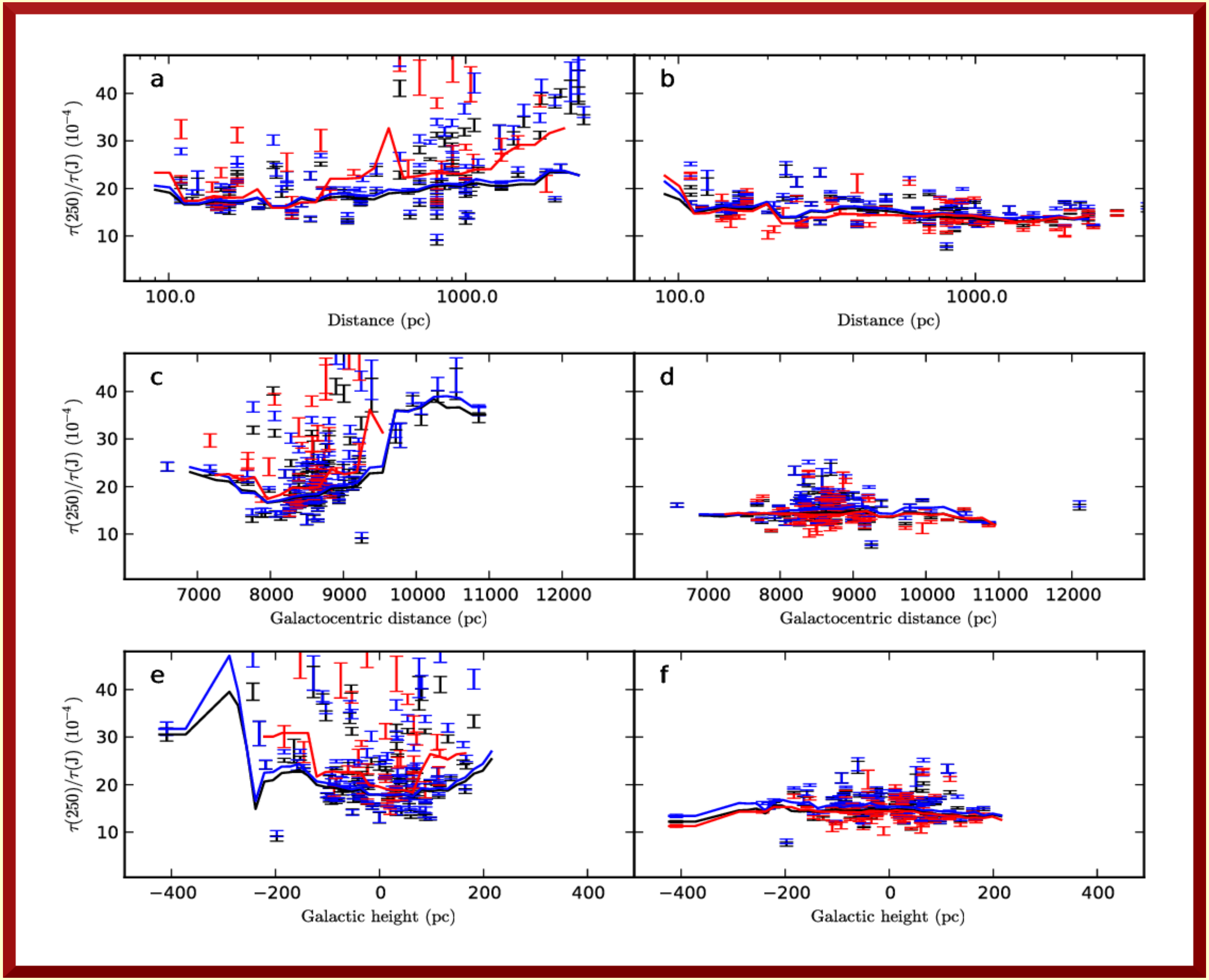

Summary

- We find for dense clumps a median ratio of
  $\tau(250\mu m)/\tau(J) = (1.6 \;\; 0.2)\times10^{-3}$,
  2-3 times the typical value in diffuse medium
- A few fields have $\tau(250\mu m)/\tau(J)$ **up to ~4×10^{-3}**
- No clear dependence on Galactic location
- **Further increase possible beyond $\tau(J)$~5**
  - large systematic errors make estimation unreliable

Results. We find a median ratio of $\tau(250\mu m)/\tau_J = (1.6 \pm 0.2) \times 10^{-3}$, which is about twice as high as the values reported for diffuse medium . No significant systematic variation is detected with Galactocentric distance or with Galactic height. The small decrease as the function of cloud distance can be attributed to selection effects or remaining bias in the τ_J values. The ratio $\tau(250\mu m)/\tau_J$ increases above $\tau_J \sim 5$ but is sensitive to the applied bias corrections. Examination of the maps of $\tau(250\mu m)/\tau_J$ reveals a handful of fields with clear signs of local increase of submillimetre opacity, up to $\tau(250\mu m)/\tau_J \sim 4 \times 10^{-3}$. These are all nearby, spatially resolved clumps with high column density.

Galactic Cold Cores VI:

Dust spectral index

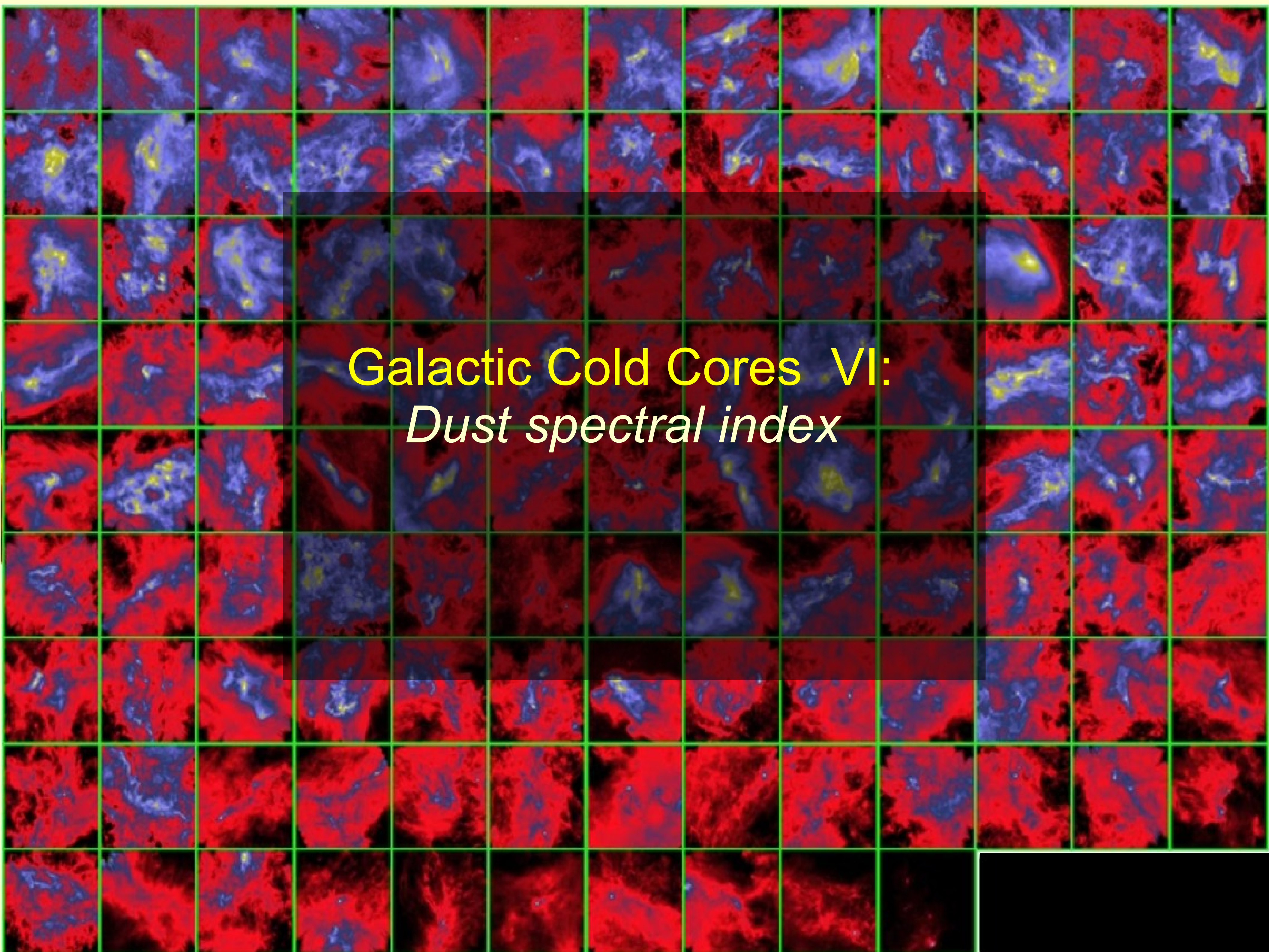

GCC sample

- **160**, **250**, **350**, and **500**µm **Herschel**
  - 100µm ignored because of **V**ery **S**mall **G**rain emission
- Planck data 857GHz – 217 GHz
- IRAS (IRIS) 100µm data

- strategy
  - measure β with Planck + IRIS
  - measure β with Herschel
  - measure β with Herschel + Planck

- **IRAS 100μm + Planck 857GHz-217GHz**
  - IRAS 100μm (IRIS) corrected for **VSG** contribution using the predictions of DustEM model (Compiègne et al. 2011)
  - 353GHz and 217GHz corrected for **CO** emission using Planck Type 3 CO map and line ratios 0.3 and 0.5
  - 217GHz corrected for **non-thermal** emission using the results of component separation (Planck 2013, XII)
  - **field averages** (all the fields!):

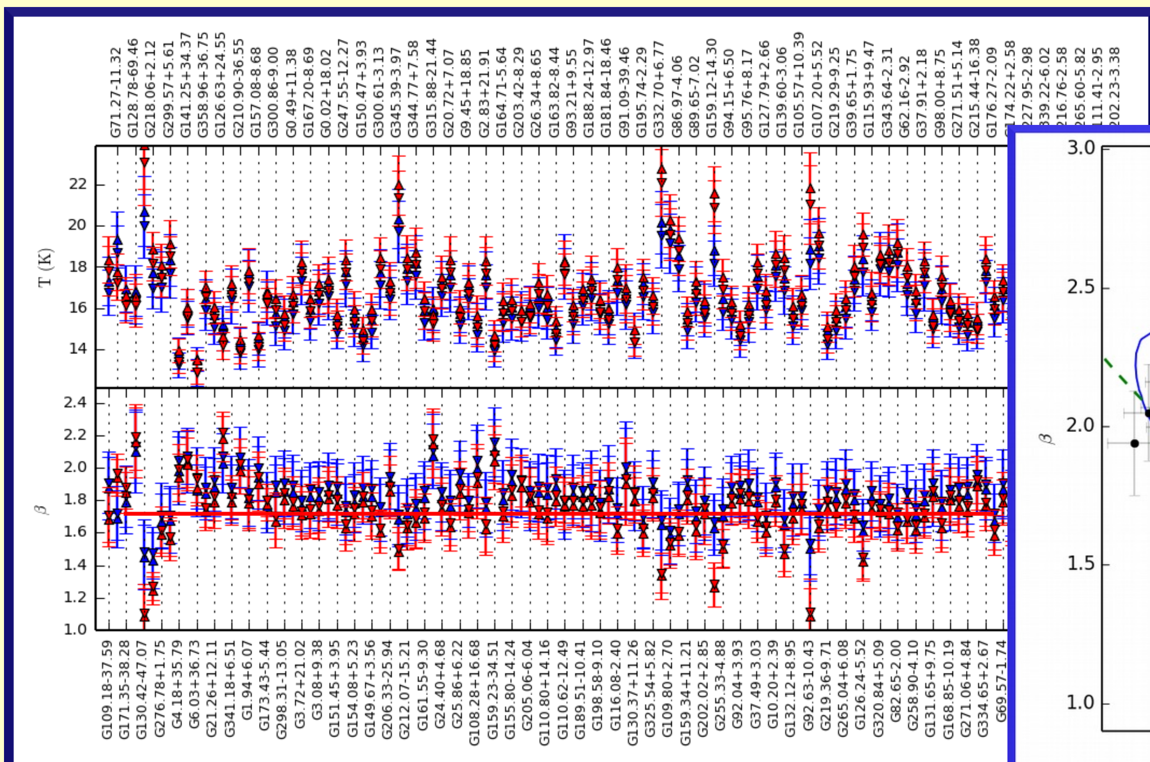

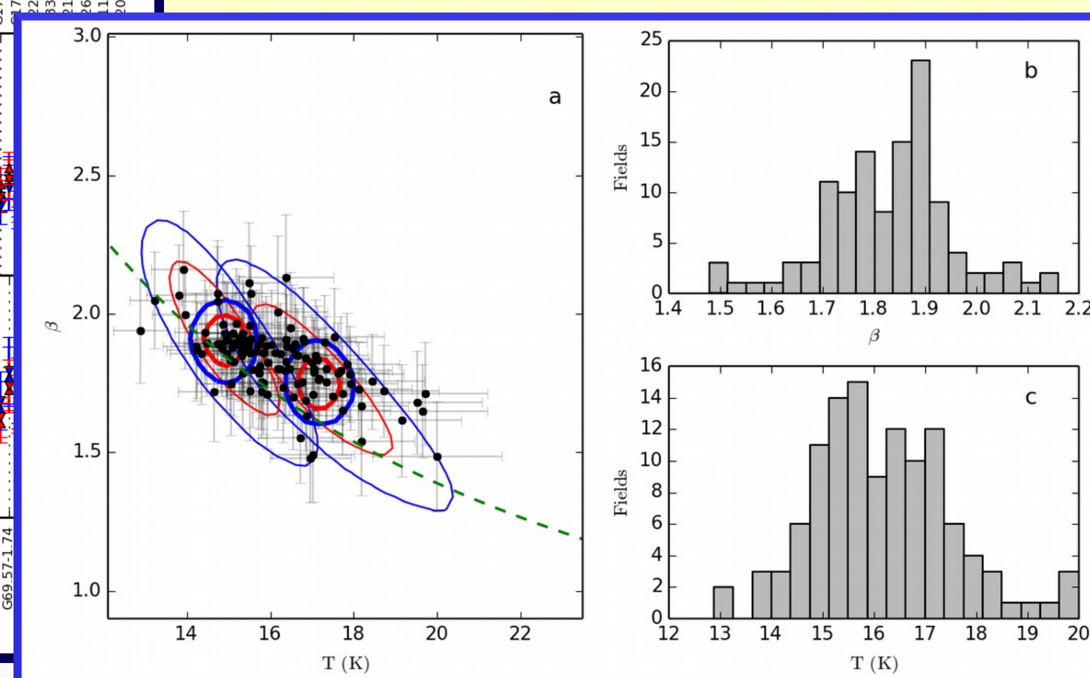

Herschel fits: 250 – 500μm, 160 – 500μm, zero point uncertainties...

LDN1642

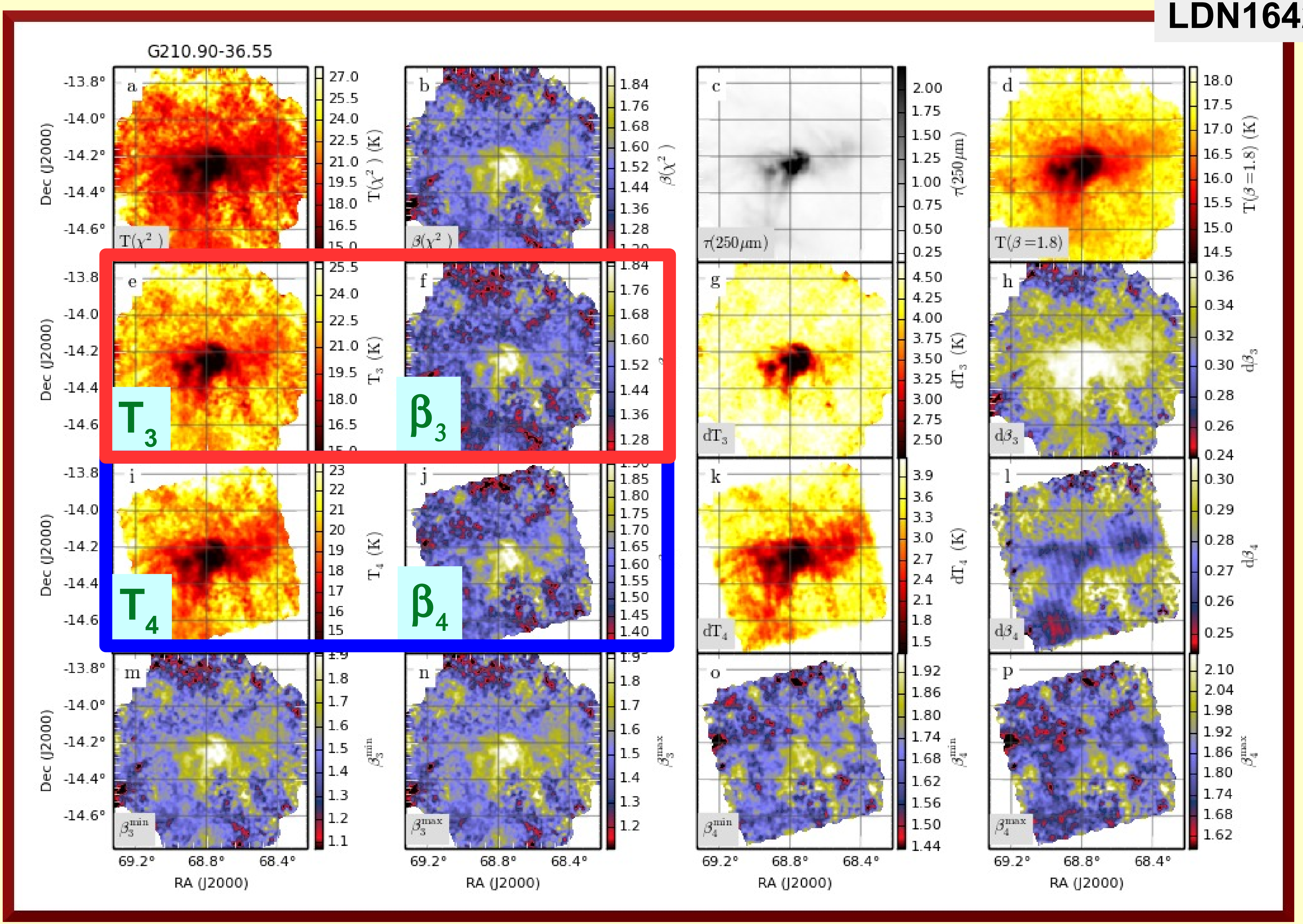

- Herschel (250-500μm) + Planck (350μm-1.4mm) **joint fits**
  - model (I_ν, T, β) defined on 28" pixels
    - fit Herschel at 38" resolution
    - simultaneous constraints from Planck at 5.0' resolution

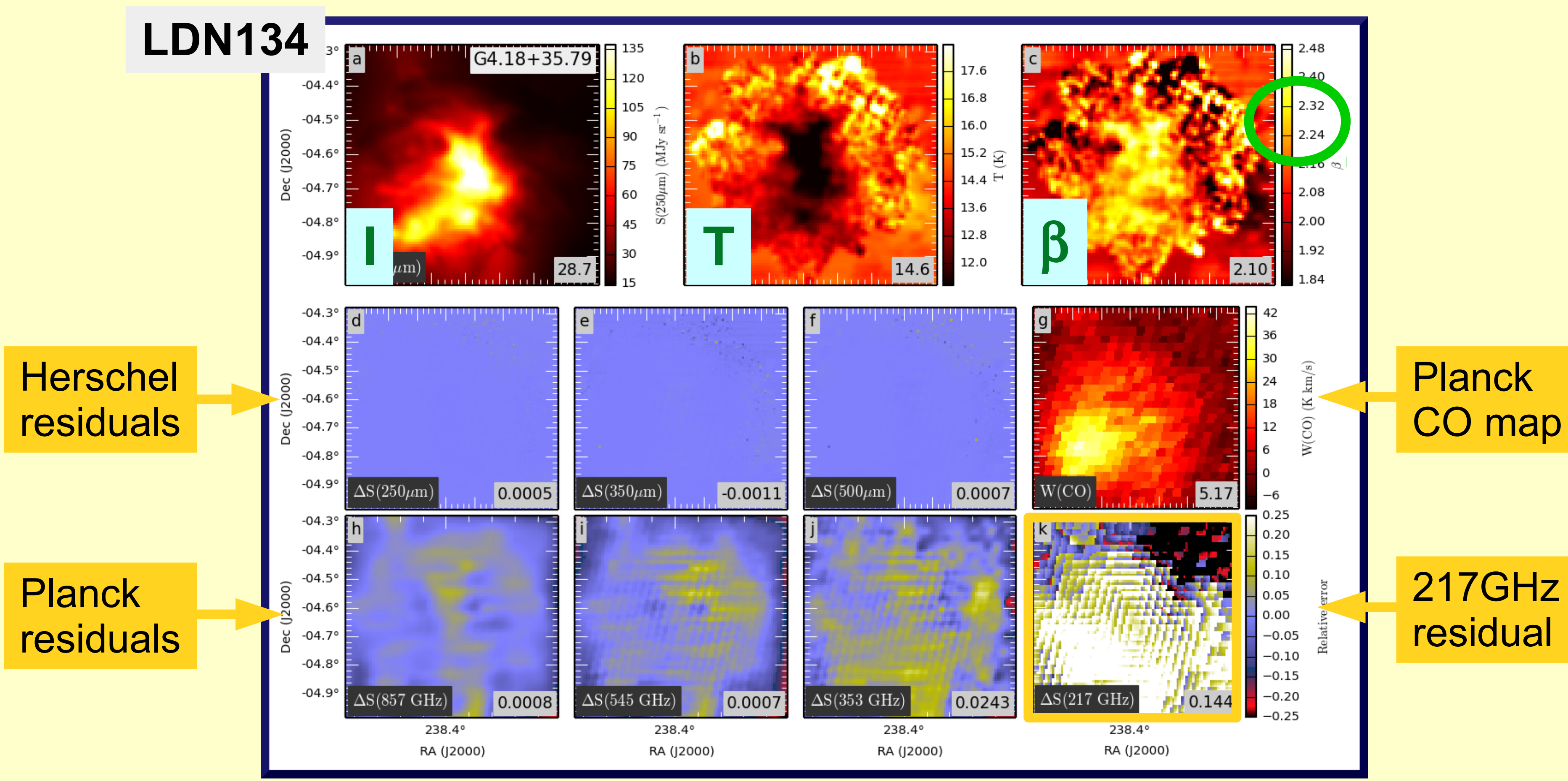

Summary

- **β ~ 1.8 or even above 2.0**, higher than molecular cloud averages
- T – β **anti-correlation** and 217GHz **excess** confirmed
  - cf “500μm excess” (Paradis et al. 2012 / Hi-GAL) and the wavelength dependence seen in Planck (2014) XVI: β_{mm}-β_{FIR}=**-0.15**
    - note: Planck allsky averages have changed following recalibration Planck (2014) XXXI: <β_{FIR}>=1.84 → **1.59** (100μm-353GHz)

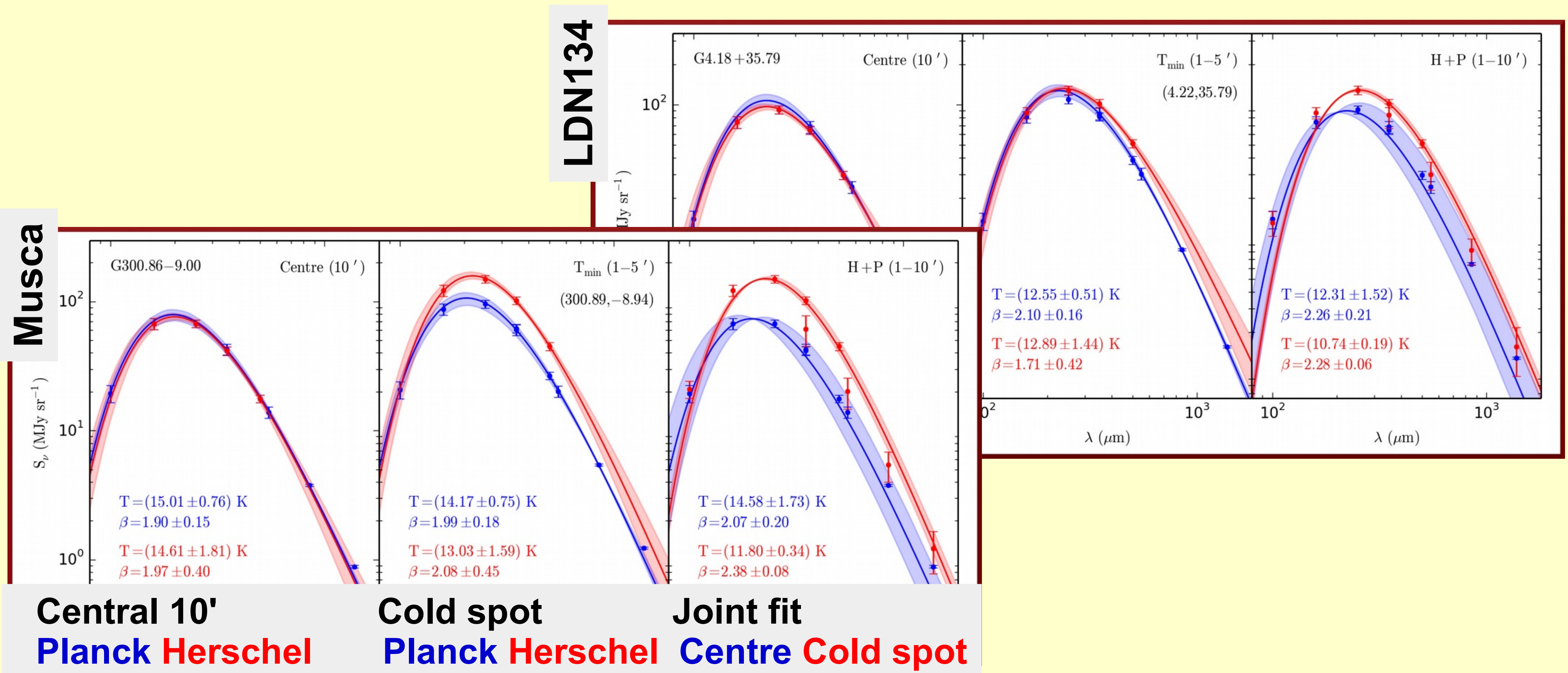

Other PGCC / Cold Cores studies ...

Spitzer programme **Hunting coreshine**

PI **R. Paladini**: 90 clumps/cores from **ECC**

- largest galactic program in cycle 8
  - 165.5 h, sensitivity 3× previous Spitzer, 10× WISE
- cycle 9 further 42.5 hours (– June 2013)
- <0.008 MJy/sr in 3.6μm and 4.5μm

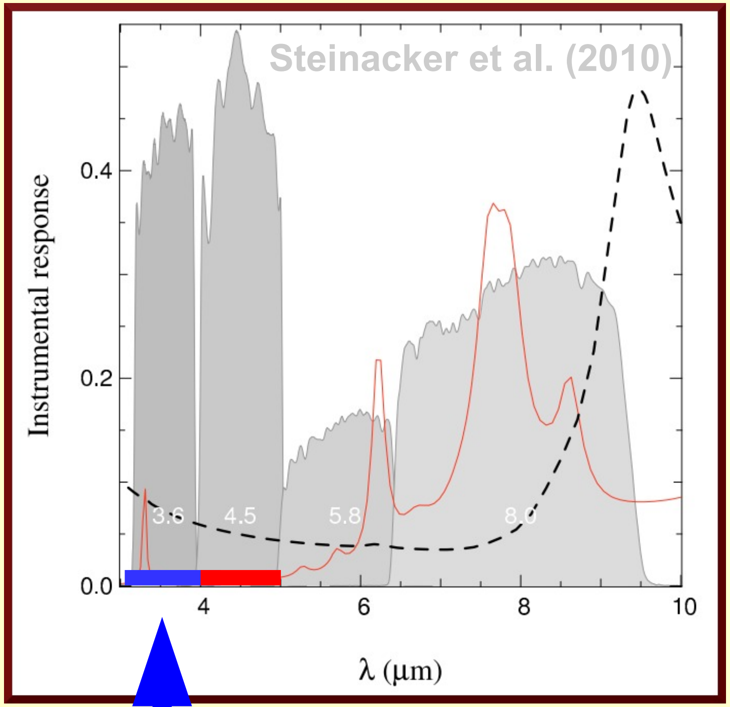

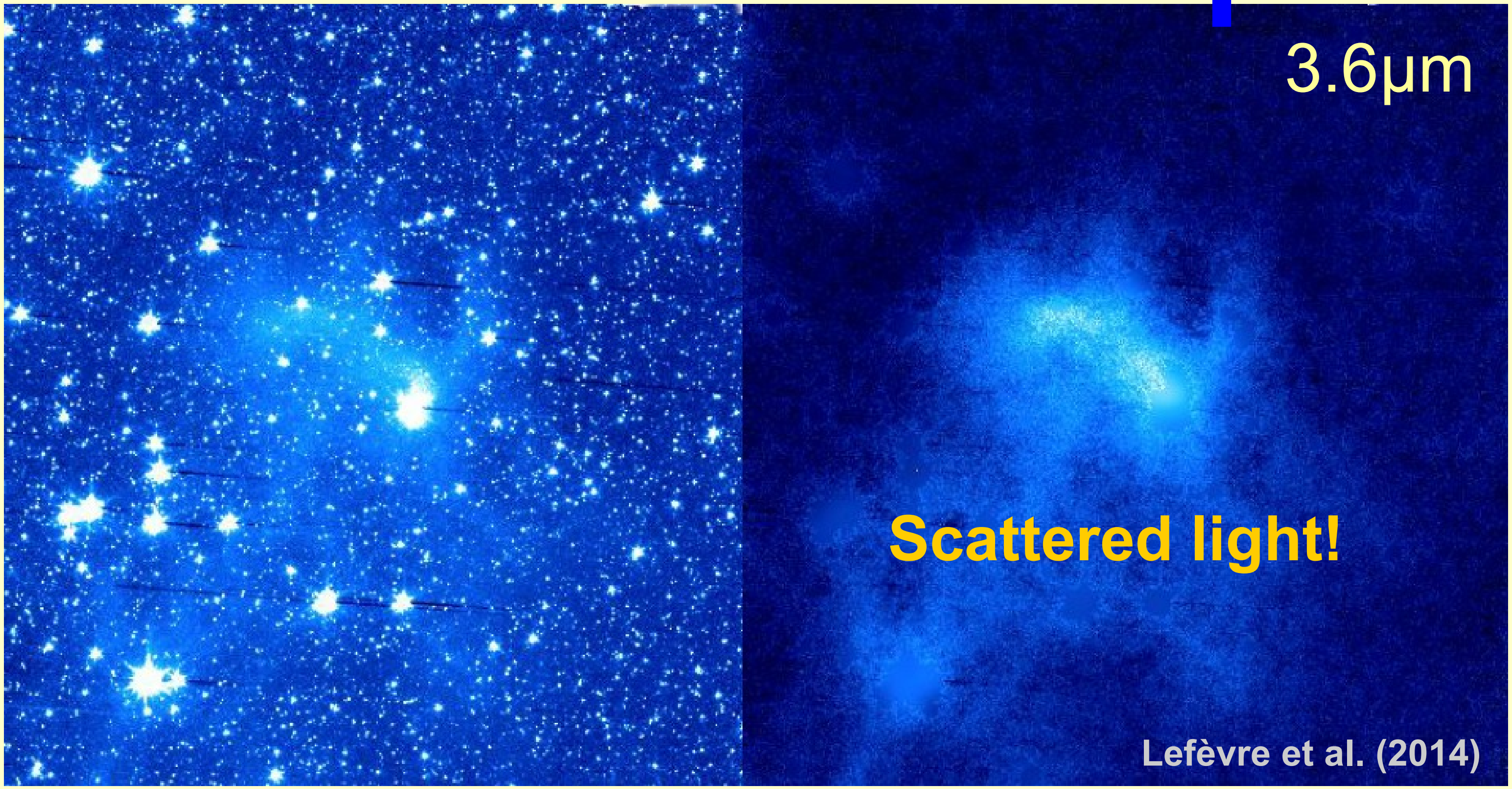

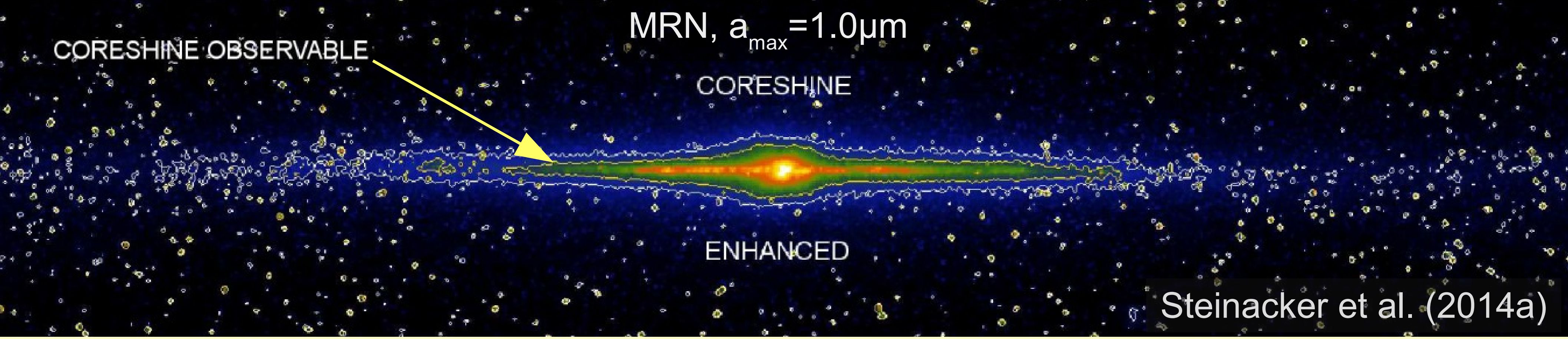

- Taurus LDN1506C: up to **~0.65μm** grains, challenging for the time scales of grain growth (Steinacker 2014b; Ysard et al. 2013)
- LDN260: a_{max}=**1.0μm**, $dn/da \sim a^{-3.65}$, 1.7 χ (Andersen et al. 2013)
- Lupus IV: similar thresholds for coreshine and **water ice** ($\tau_{9.7\mu m}$>0.15)
  - ice mantles have a strong effect on albedo (Andersen et al. 2014)
- **Saajasto et al. (in prep.)**

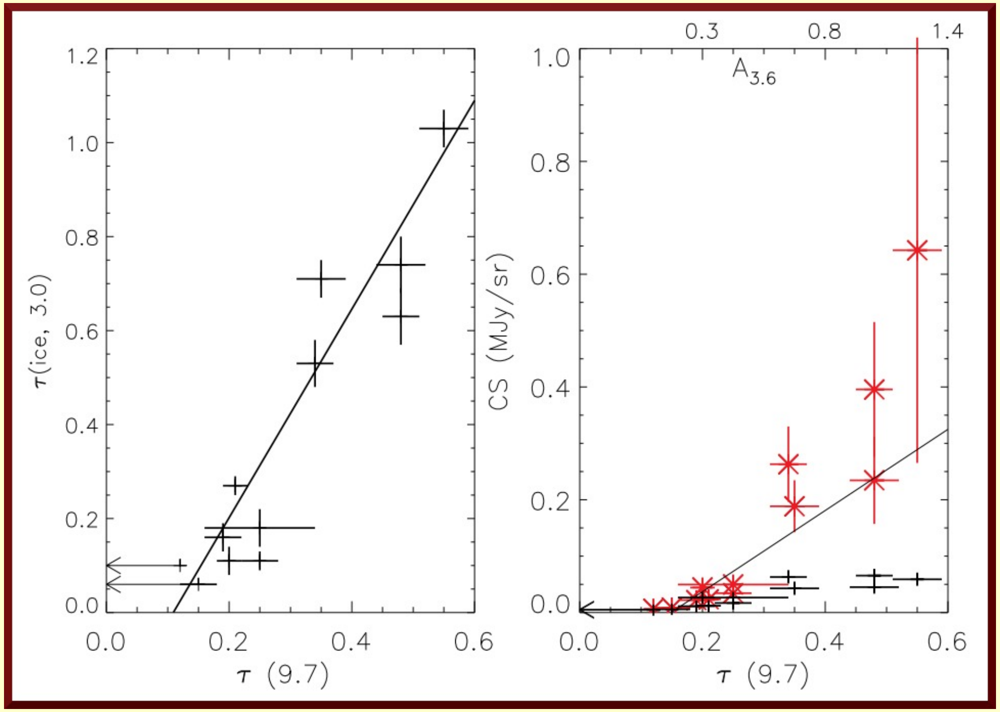

Planck: polarisation

- sub-mm dust **polarisation**
  - grains aligned in the B field
  - maps of field geometry, even field strength
- first Planck papers: large scales, down to individual cloud filaments
- work **on PGCC**
  - stacking analysis, density vs. magnetic field structure

Planck intermediate results. XXXV (2015)

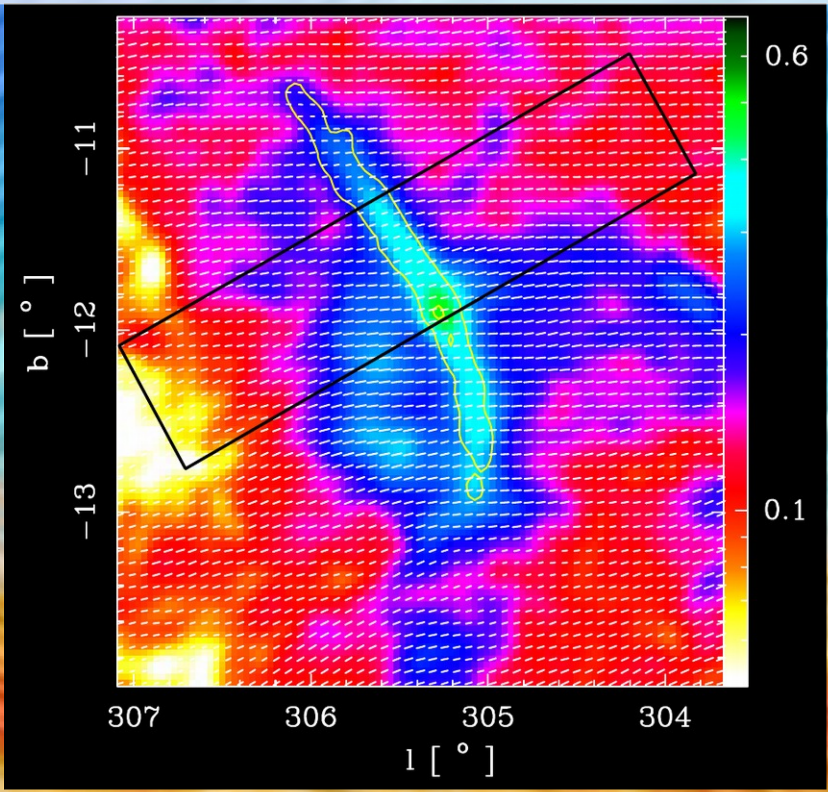

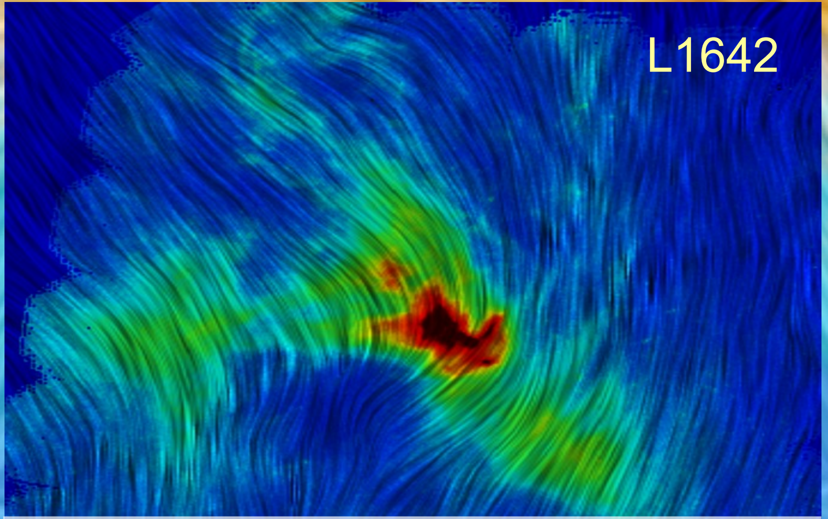

Malinen et al. (2016)

ESA/Planck Collaboration. M.-A. Miville-Deschênes (IAS)

GCC-X: Clump structure

- work in progress
  - density structure of individual clumps
    - radial **profile** and 2D shape: **elongation**, **orientation**
    - use modelling to evaluate the uncertainties from radiative transfer effects and dust properties
    - use model density distribution to estimate **stability**?
  - compare clump orientation to general **field anisotropy** at different scales
    - use *template matching* to identify elongated structures at different scales

Field	RA (J2000.0)	DEC (J2000.0)	Distance (pc)	Size (arcmin)	Model size (pixels)	A_V^{BG} (mag)	R (arcmin)	p
(1)	(2)	(3)	(4)	(5)	(6)	(7)	(8)	(9)
G358.96+36.75	15 39 50.0	-07 12 09.0	110	35.1	234×234	0.2	1.8	2.2
G6.03+36.73	15 54 05.9	-02 54 39.7	110	35.1	234×234	0.4	0.7	2.2
G141.25+34.37	08 48 58.2	+72 41 16.1	110	40.0	267×267	0.1	1.2	1.8
G4.18+35.79	15 53 43.4	-04 40 55.9	110	35.1	234×234	0.5	2.7	3.6
G21.26+12.11	17 46 47.7	-04 38 48.1	120	35.1	234×234	0.9	0.5	2.3
G126.63+24.55	04 19 14.0	+85 52 06.5	125	30.0	200×200	0.2	2.3	4.6
G210.90-36.55	04 34 54.6	-14 23 35.1	140	50.1	334×334	0.5	4.0	5.3
G341.18+6.51	16 25 05.1	-39 59 10.4	140	25.1	167×167	1.4	3.2	6.2
G1.94+6.07	17 27 50.7	-24 01 54.2	145	40.0	267×267	1.6	11.5	8.1
PCC550	12 25 17.0	-71 43 05.5	150	36.0	240×240	0.7	1.3	3.1
G298.31-13.05	11 39 22.1	-75 14 27.0	150	25.1	167×167	0.5	1.1	2.6
G157.08-8.68	04 01 55.7	+41 15 20.4	150	40.0	267×267	1.1	0.5	2.1
G173.43-5.44	05 08 32.7	+31 26 38.8	150	45.0	300×300	0.9	1.5	2.5
G3.72+21.02	16 39 45.9	-14 02 09.3	160	40.0	267×267	0.6	0.6	1.8
G0.49+11.38	17 04 41.9	-22 13 52.3	160	35.1	234×234	0.7	1.3	3.3
G167.20-8.69	04 36 34.8	+34 16 53.3	160	40.0	267×267	0.9	0.5	1.8
G3.08+9.38	17 17 29.6	-21 22 16.4	160	42.0	280×280	0.7	1.1	1.8
G0.02+18.02	16 40 56.7	-18 35 03.7	160	28.1	187×187	0.5	2.9	2.4
G154.08+5.23	04 47 34.4	+53 05 02.4	170	34.0	227×227	1.2	0.5	2.4
G151.45+3.95	04 29 53.9	+54 16 52.5	170	36.0	240×240	1.2	3.5	2.6
G150.47+3.93	04 24 37.8	+54 58 21.4	170	40.0	267×267	1.7	0.3	1.9
G149.67+3.56	04 17 53.6	+55 15 05.2	170	40.0	267×267	1.6	1.5	2.2
G247.55-12.27	07 09 26.3	-36 16 39.6	170	44.1	294×294	0.5	1.9	2.0
G300.61-3.13	12 28 54.8	-65 47 40.5	200	36.0	240×240	1.2	1.9	3.0
G206.33-25.94	05 07 01.2	-06 17 56.6	210	35.1	234×234	0.1	0.8	2.6
G345.39-3.97	17 23 01.0	-43 26 24.7	225	33.0	220×220	0.9	0.5	3.0
G212.07-15.21	05 55 49.7	-06 11 25.9	230	36.0	240×240	0.6	1.3	2.0
G344.77+7.58	16 33 30.3	-36 39 02.1	240	40.0	267×267	0.9	0.5	2.4
G161.55-9.30	04 16 06.1	+37 49 20.2	250	36.0	240×240	0.8	0.8	2.0
G315.88-21.44	17 19 39.9	-76 55 17.2	250	35.1	234×234	0.2	0.7	2.2
G20.72+7.07	18 03 38.9	-07 30 25.0	260	30.0	200×200	1.3	0.8	1.8
G25.86+6.22	18 16 32.7	-03 23 49.4	260	36.0	240×240	3.1	0.6	1.9
G24.40+4.68	18 19 21.5	-05 29 45.1	260	36.0	240×240	1.7	0.8	2.1
G9.45+18.85	17 00 22.2	-10 53 06.1	280	40.0	267×267	0.6	4.7	2.9
G2.83+21.91	16 34 41.2	-14 09 27.4	300	38.1	254×254	0.6	1.8	2.1
G108.28+16.68	21 10 13.4	+72 52 58.5	300	35.1	234×234	0.6	0.9	2.1
G159.23-34.51	02 55 54.0	+19 37 10.2	325	40.0	267×267	0.6	0.8	2.0
G164.71-5.64	04 40 58.0	+37 59 06.6	330	42.0	280×280	1.3	1.2	1.9
G155.80-14.24	03 36 49.2	+37 42 31.1	350	40.0	267×267	0.5	0.6	2.1
G203.42-8.29	06 04 47.6	+04 20 31.3	390	44.1	294×294	0.7	1.6	3.6
G26.34+8.65	18 08 37.9	-01 51 26.6	400	30.0	200×200	1.3	1.0	3.6
G205.06-6.04	06 16 27.5	+04 07 44.0	400	44.1	294×294	0.8	1.3	2.1
G110.80+14.16	21 59 02.5	+72 52 56.0	400	40.0	267×267	0.7	0.5	1.9
G163.82-8.44	04 29 00.9	+36 43 21.1	420	50.1	334×334	1.4	0.4	2.1
G93.21+9.55	20 37 00.2	+56 58 46.8	440	30.0	200×200	0.9	0.4	2.5
G110.62-12.49	23 37 39.8	+48 31 40.4	440	40.0	267×267	0.2	0.6	2.6
G188.24-12.97	05 17 05.1	+14 59 33.2	445	40.0	267×267	0.6	0.8	1.6
G189.51-10.41	05 29 55.2	+15 25 03.2	445	42.0	280×280	0.6	0.5	2.1
G198.58-9.10	05 52 53.1	+08 22 34.1	450	35.1	234×234	0.7	1.1	4.0
G116.08-2.40	23 57 06.7	+59 43 26.9	500	30.0	200×200	1.3	0.8	2.3
G181.84-18.46	04 44 00.3	+16 57 22.7	500	36.0	240×240	0.7	1.4	2.8

The sample:
51 fields at distances <500pc

Table 2. Parameters of the default radiative transfer models and the changes in the assumptions for the alternative fits

Variation	Assumptions
default	$\tau(250\mu m)/\tau(J) = 1.0\times10^{-3}$, $\beta = 1.8$
P	k_{ISRF} fitted using pixels with highest 3% of $N(H_2)$
W	line-of-sight cloud extent adjusted pixel by pixel
ΔA_V	external field changed by $A_V = \pm 1$ mag
K	$\tau(250\mu m)/\tau(J) = 2.0\times10^{-3}$, $\beta = 2.1$
TD	dust changes with density from *def*. to K

Radiative transfer models
→ better estimates of
column density (variations)?

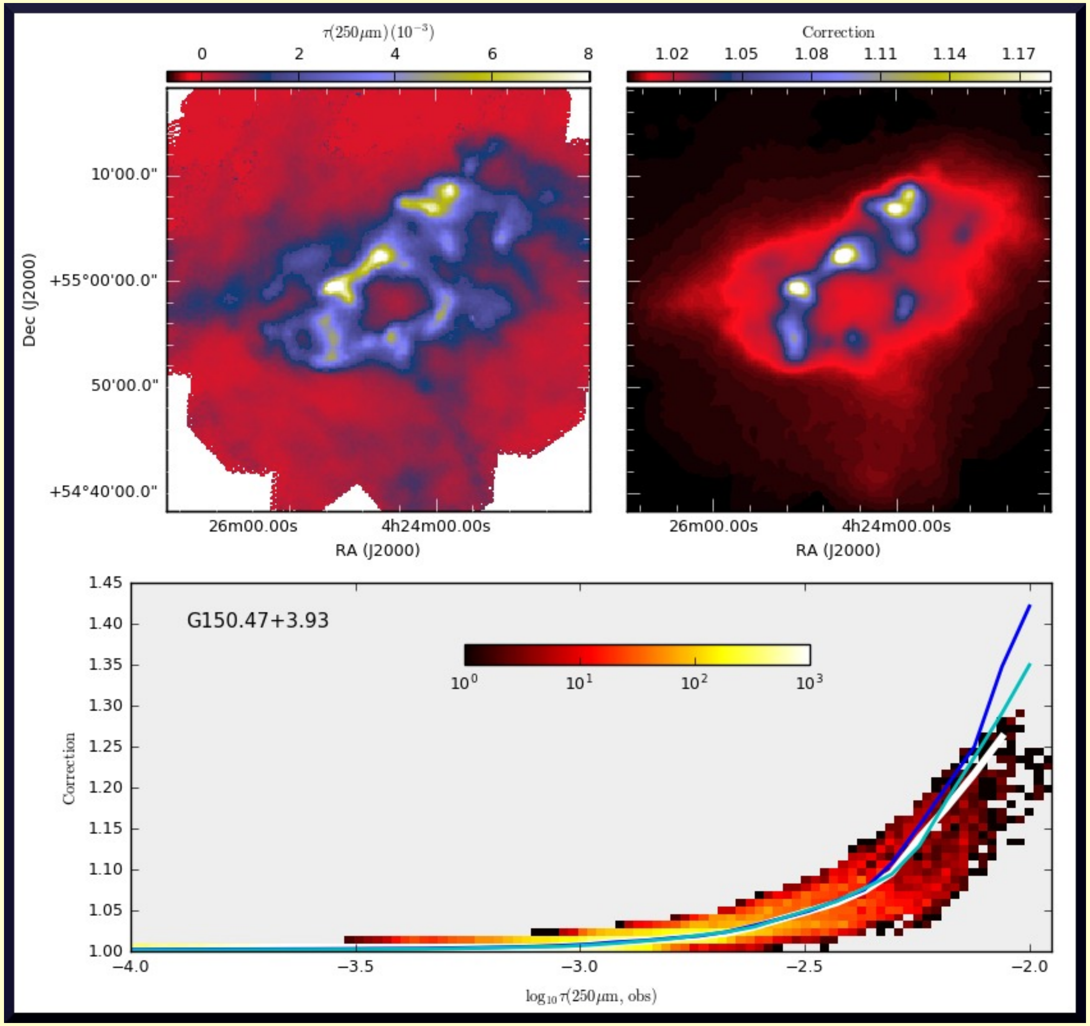

Estimates of the radiation field

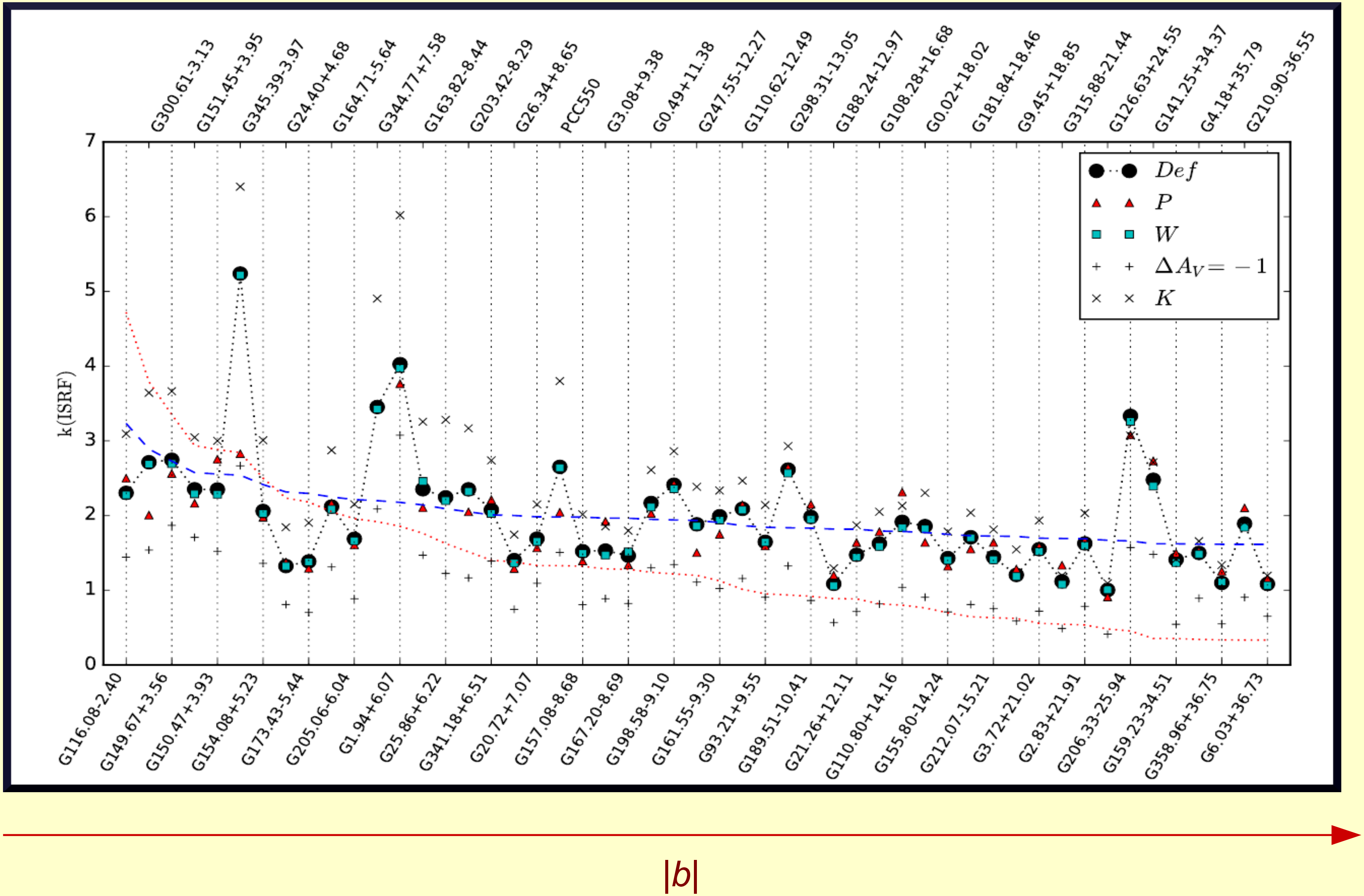

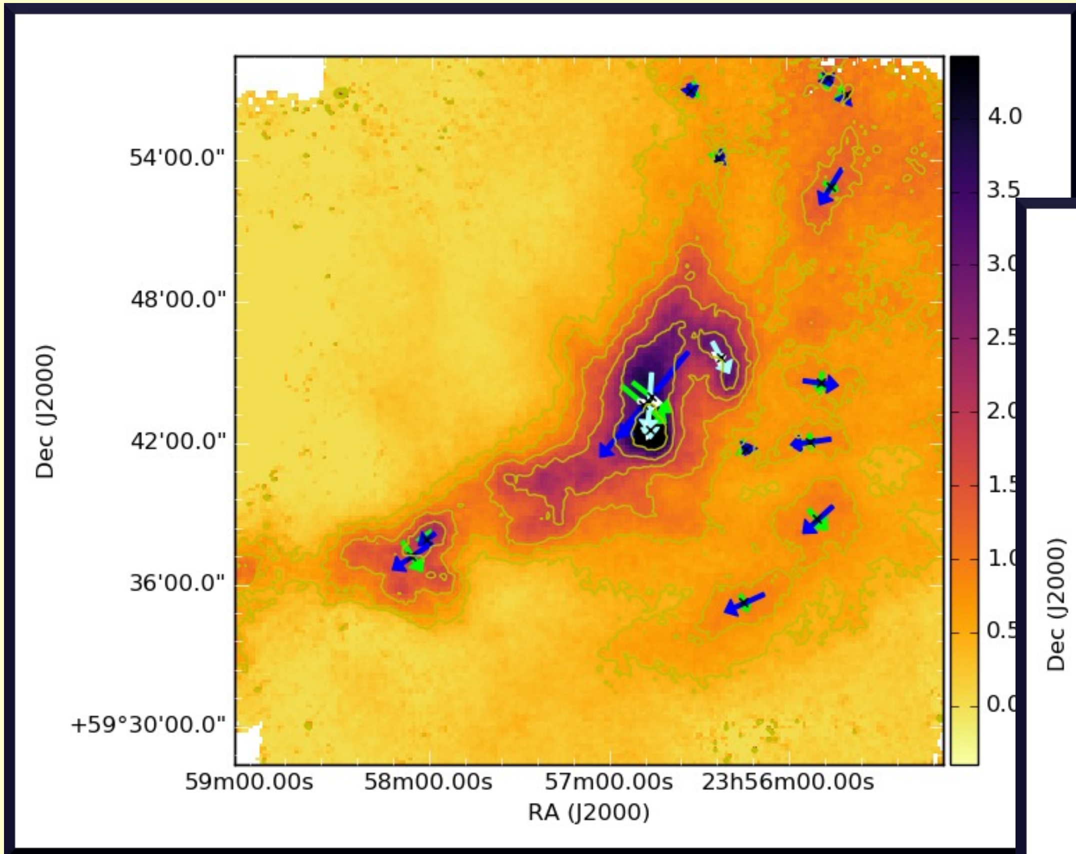

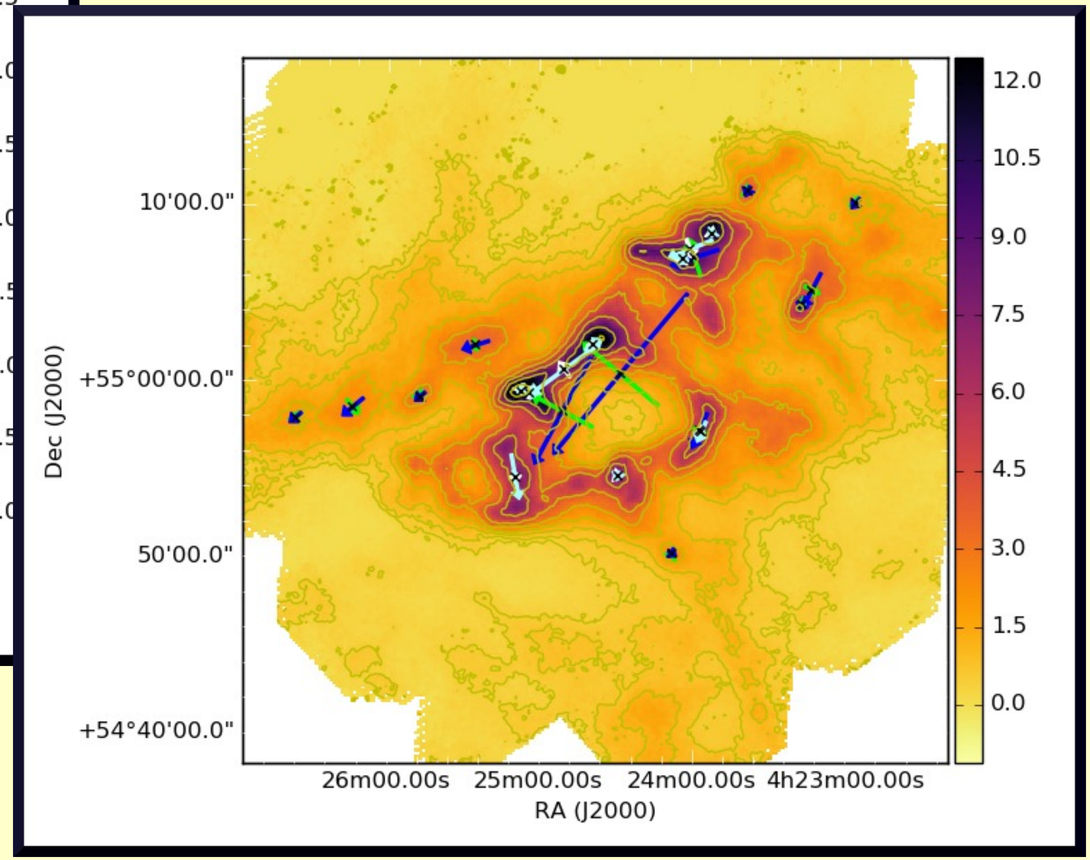

2D Gaussian and Plummer fits

Clump orientations vs.
general structural anisotropy of the fields?

Template matching
– a general tool for to analyse map structure?

(submitted)

- The simplest way to search for patterns in image data?
  - Create a **template** of the pattern and **match** it to data for different *positions*, *scales*, and position *angles* θ
  - Template is a small image T_{ij} and the best match is quantified by its **θ** and the **significance** S=sum(T_{ij} D_{ij})
    - D_{ij} are data values "under" the template elements
    - True statistical significance of S from Monte Carlo

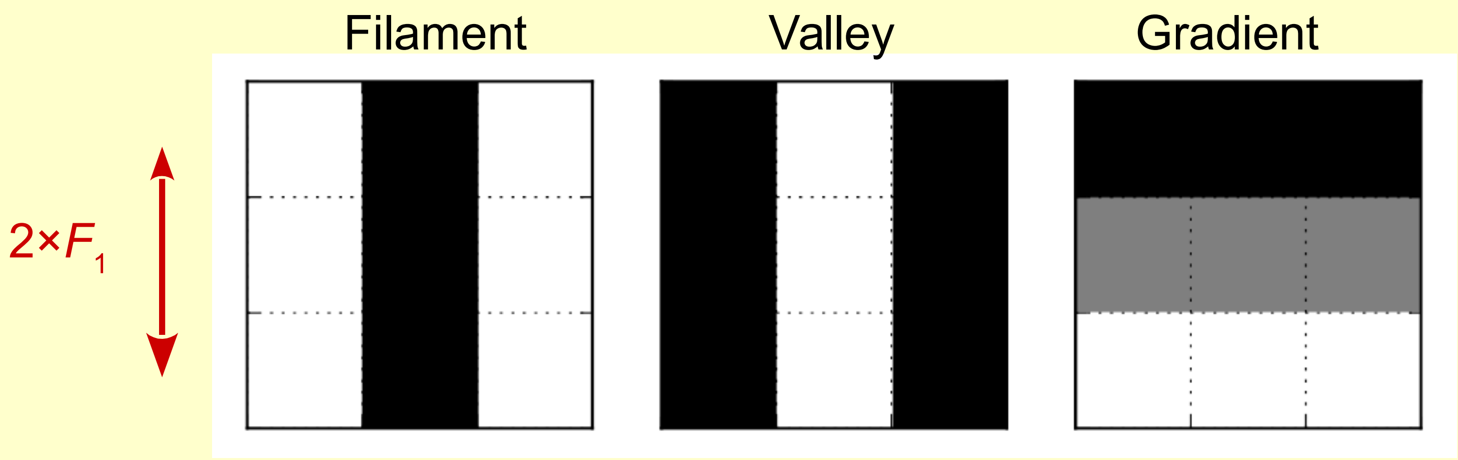

Data high-pass **filtered** with FWHM=F_1, low-pass filtered with F_2

- concentrate on a given *scale*

If data are **normalised**, significance depends on the similarity of the structures (template vs. data) not the absolute values

- good for *faint* regions

Right: “filaments” in **Musca**

- templates at 40" and 5' resolution
- *skeletons* trace regions of high *S* (uppermost 20%) and coherent θ
- the faintest features are still “real”, features in the data
  - $N(H_2)$~10^{20} cm^{-3}

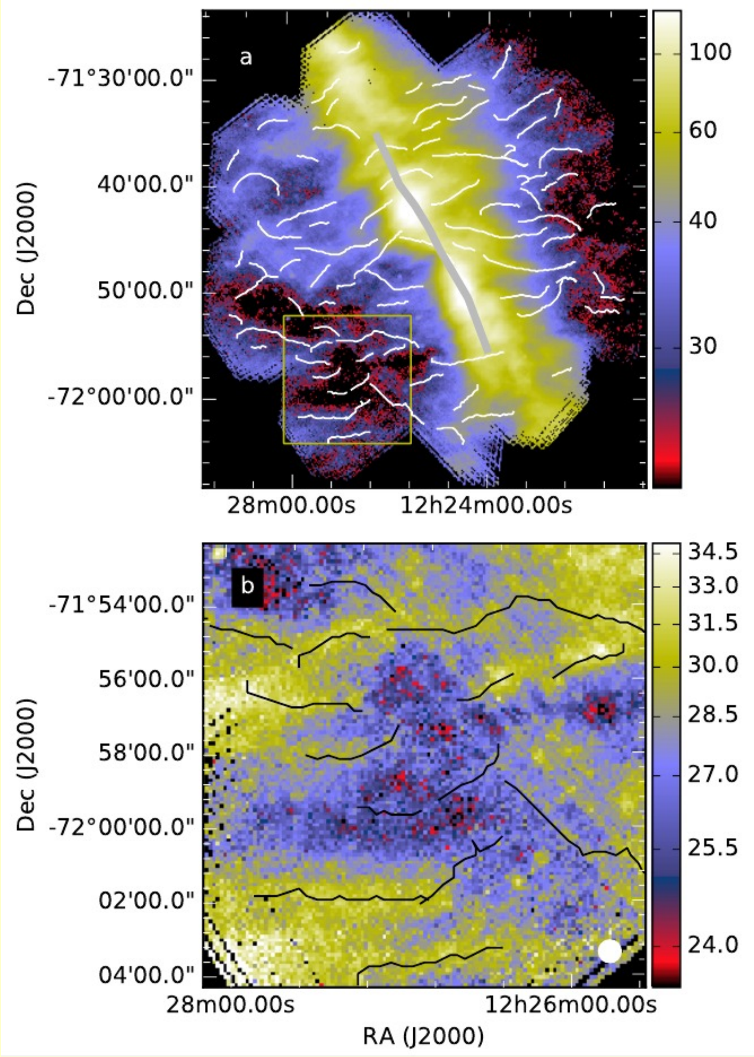

S and θ independent for every pixel position

- any coherence in *S* and θ *is* from data!
  - *skeletons are post processing…*
- fast = ~1s for images such as **L1642** (cf. Malinen et al. 2014, 2016)

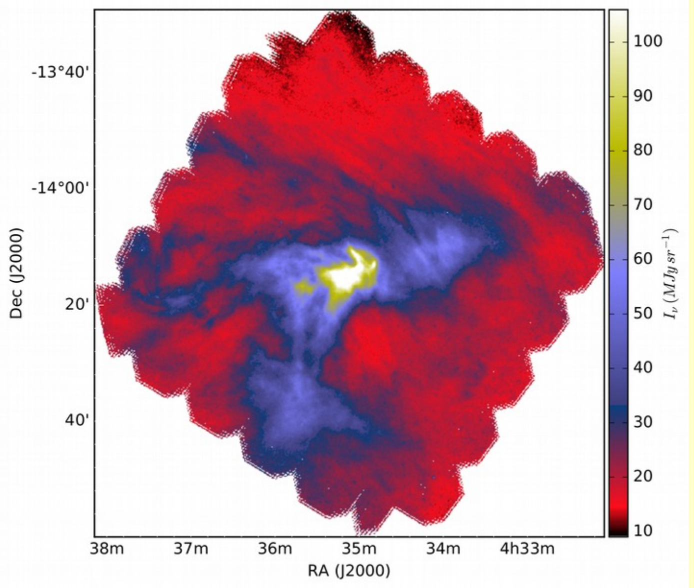

Scale: 1 arcmin

Scale: 2 arcmin

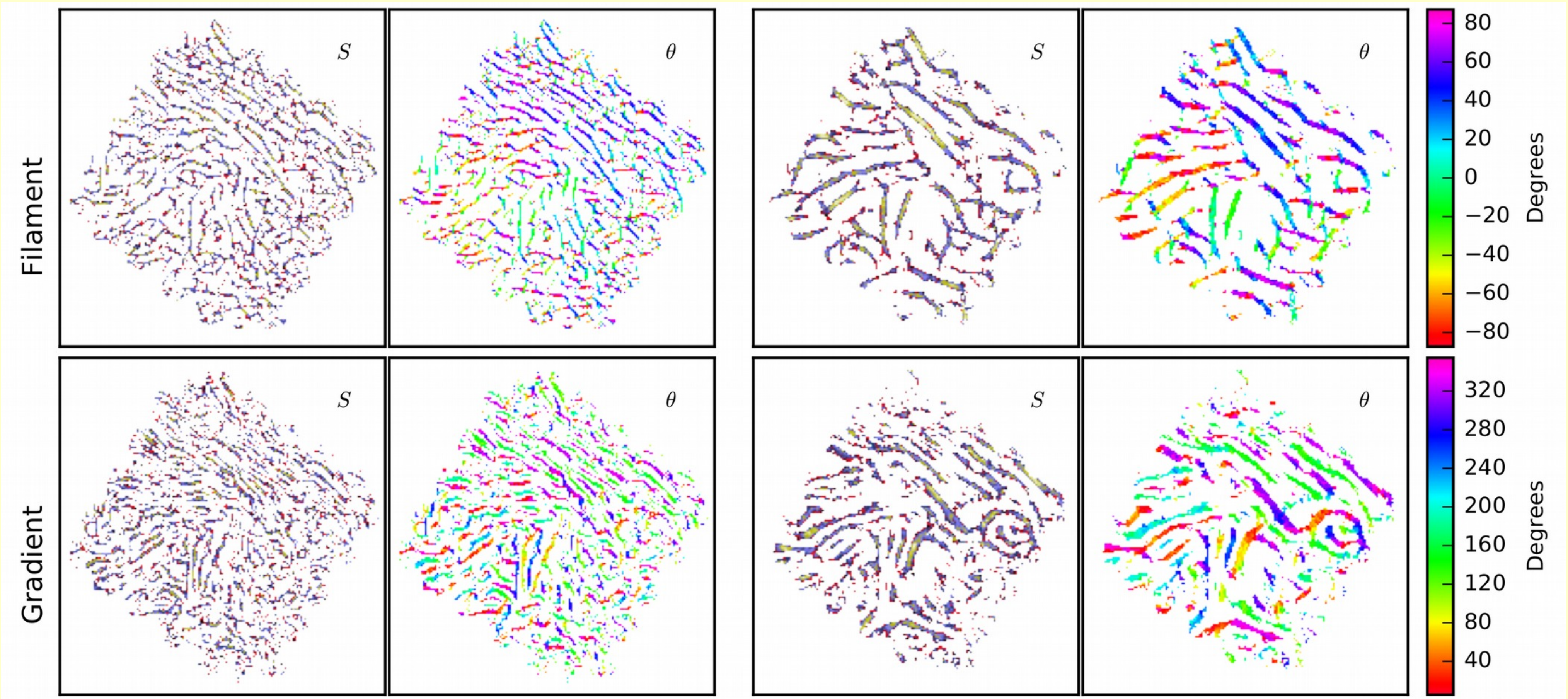

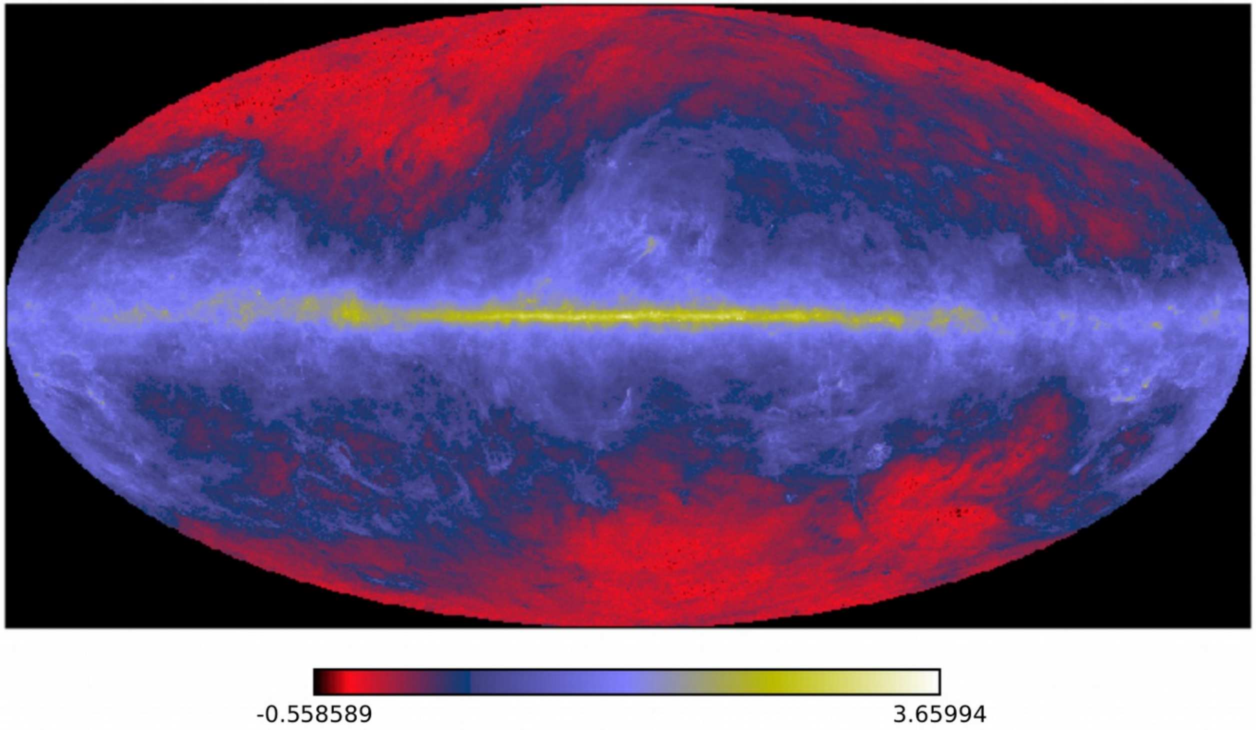

Planck 857GHz,
~50 million pixels...

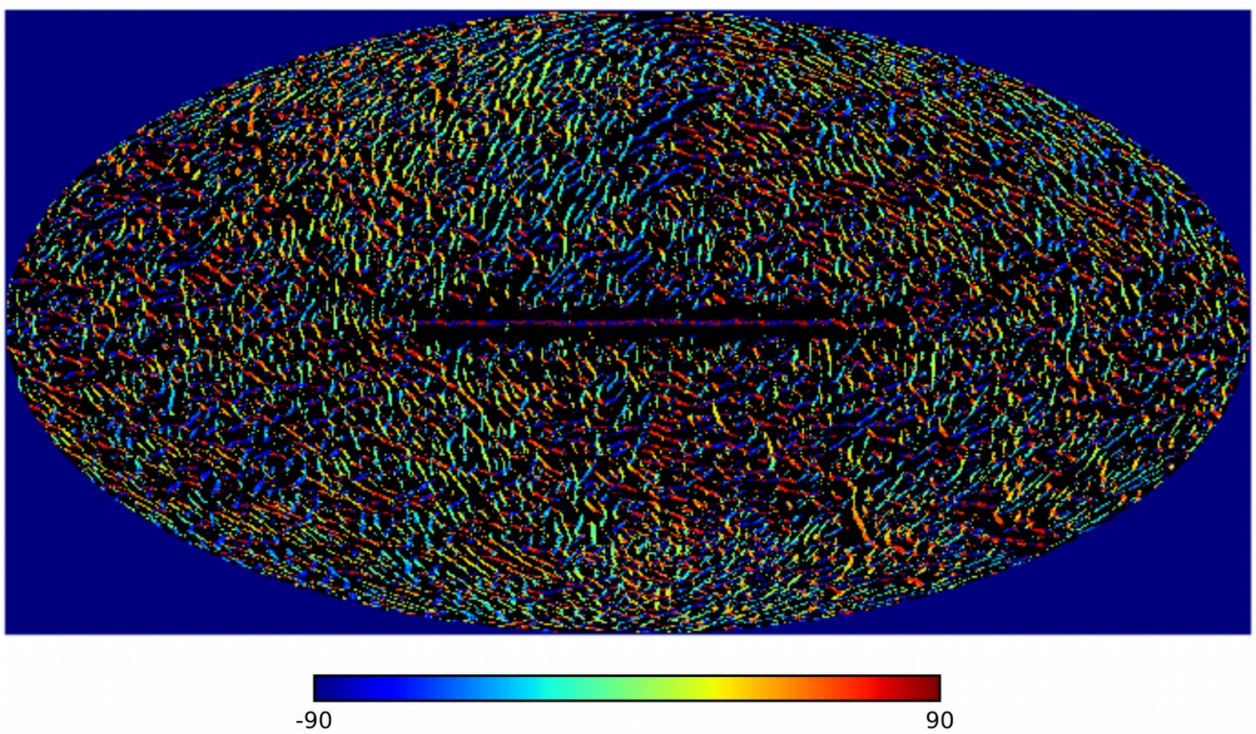

Filament template,
F_1 = 2°, F_2=6°

- θ plotted for pixels with *S* in the uppermost 10%
- calculation ~20 sec...

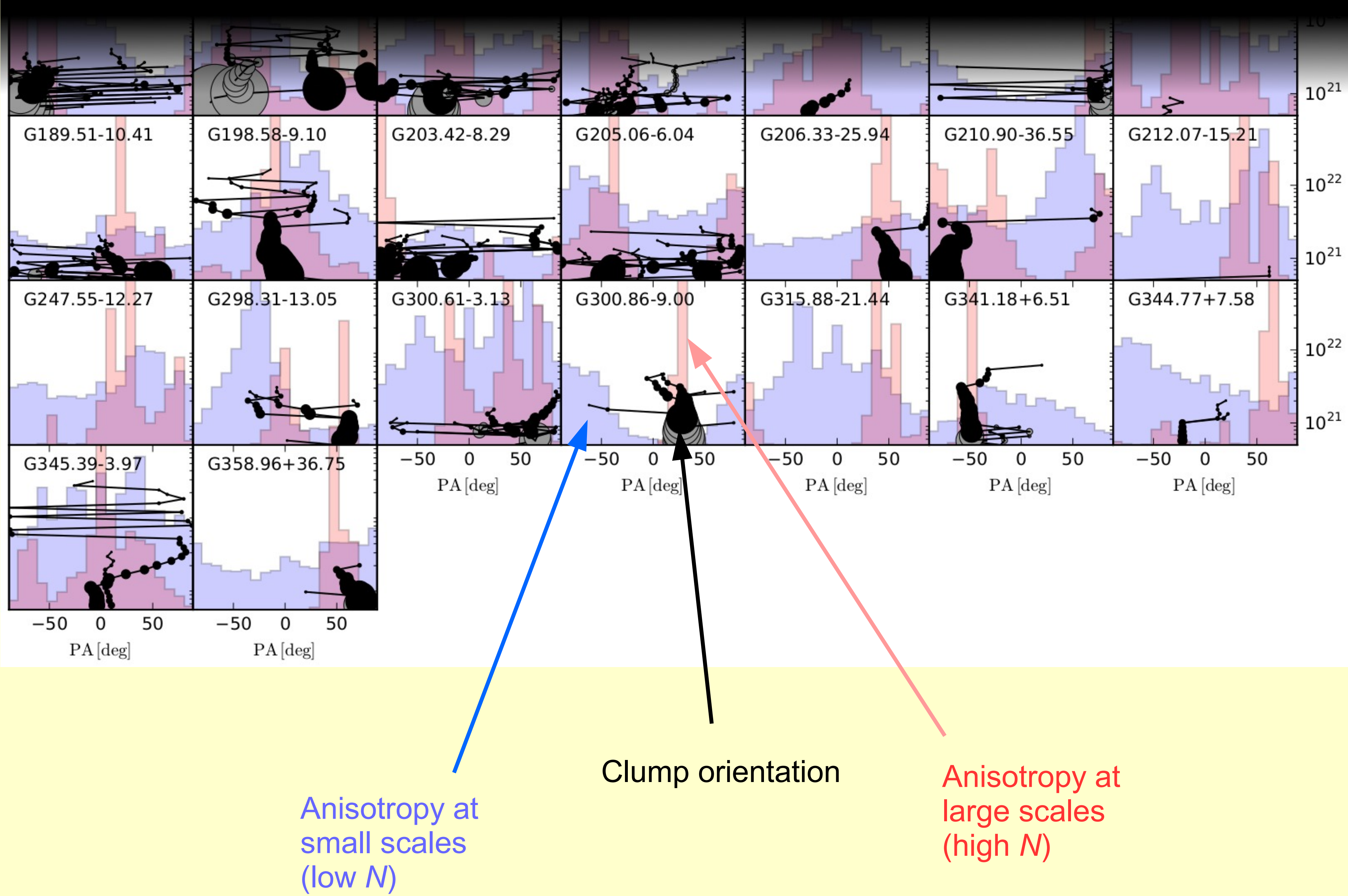
G189.51-10.41
G198.58-9.10
G203.42-8.29
G205.06-6.04
G206.33-25.94
G210.90-36.55
G212.07-15.21
G247.55-12.27
G298.31-13.05
G300.61-3.13
G300.86-9.00
G315.88-21.44
G341.18+6.51
G344.77+7.58
G345.39-3.97
G358.96+36.75
10^{21}
10^{22}
PA [deg]
−50 0 50
Anisotropy at small scales (low N)
Clump orientation
Anisotropy at large scales (high N)

→ **GCC-X**

NIR extinction

- Extinction = **temperature-independent** mass estimate
- (1) All-sky map of NICER & NICEST extinction (2MASS)
  - Healpix maps (NSIDE=2048 – 4096) @ 3.0', 4.5', 12.0'
- (2) For the statistics of intrinsic stellar colours, should one go beyond the covariance matrix description?
  - rarely, unless one has extremely precise photometry
  - knowledge of the **small scale structure** in column density can significantly reduce the noise

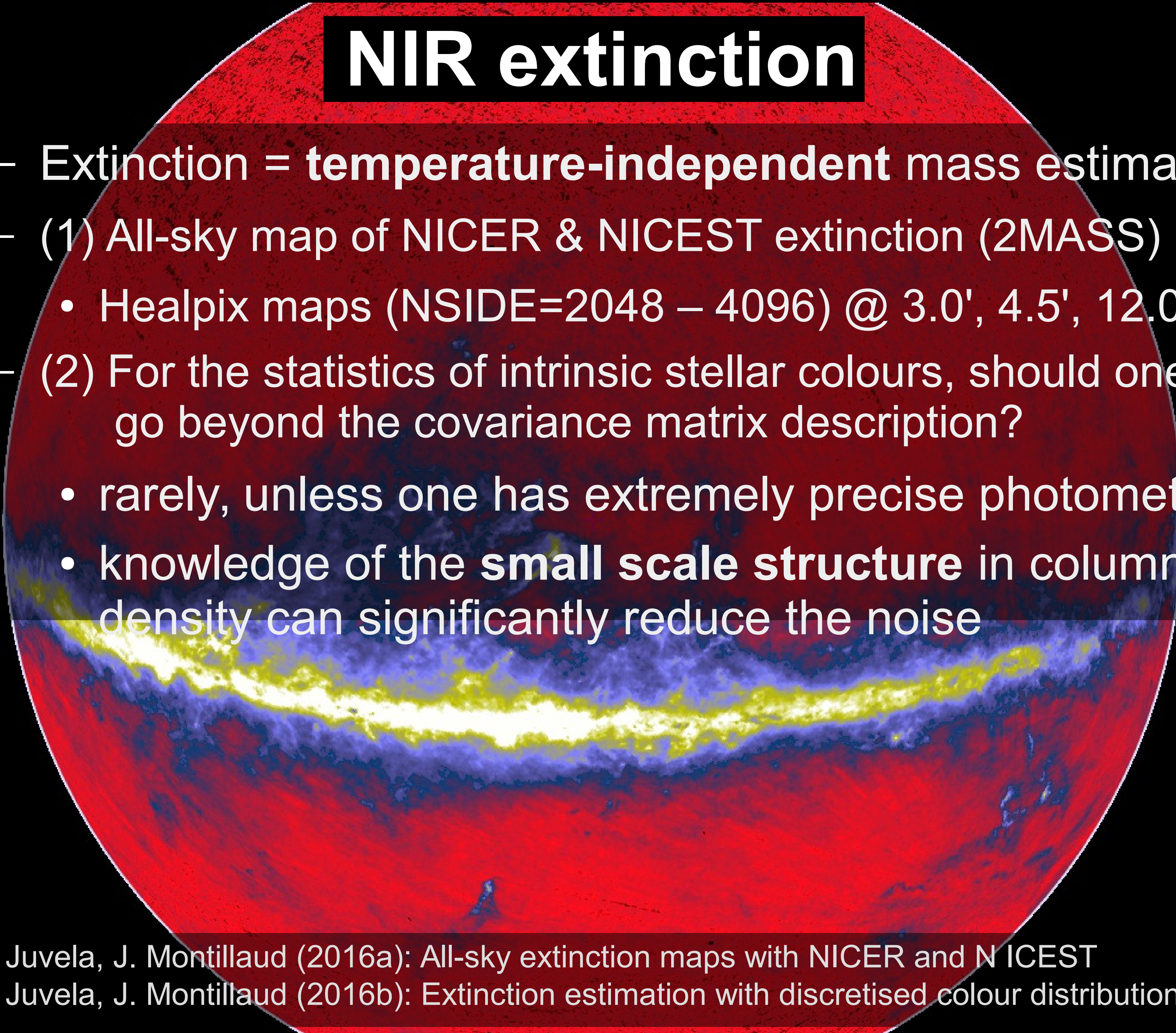

M. Juvela, J. Montillaud (2016a): All-sky extinction maps with NICER and N ICEST
M. Juvela, J. Montillaud (2016b): Extinction estimation with discretised colour distributions

www.interstellarmedium.org

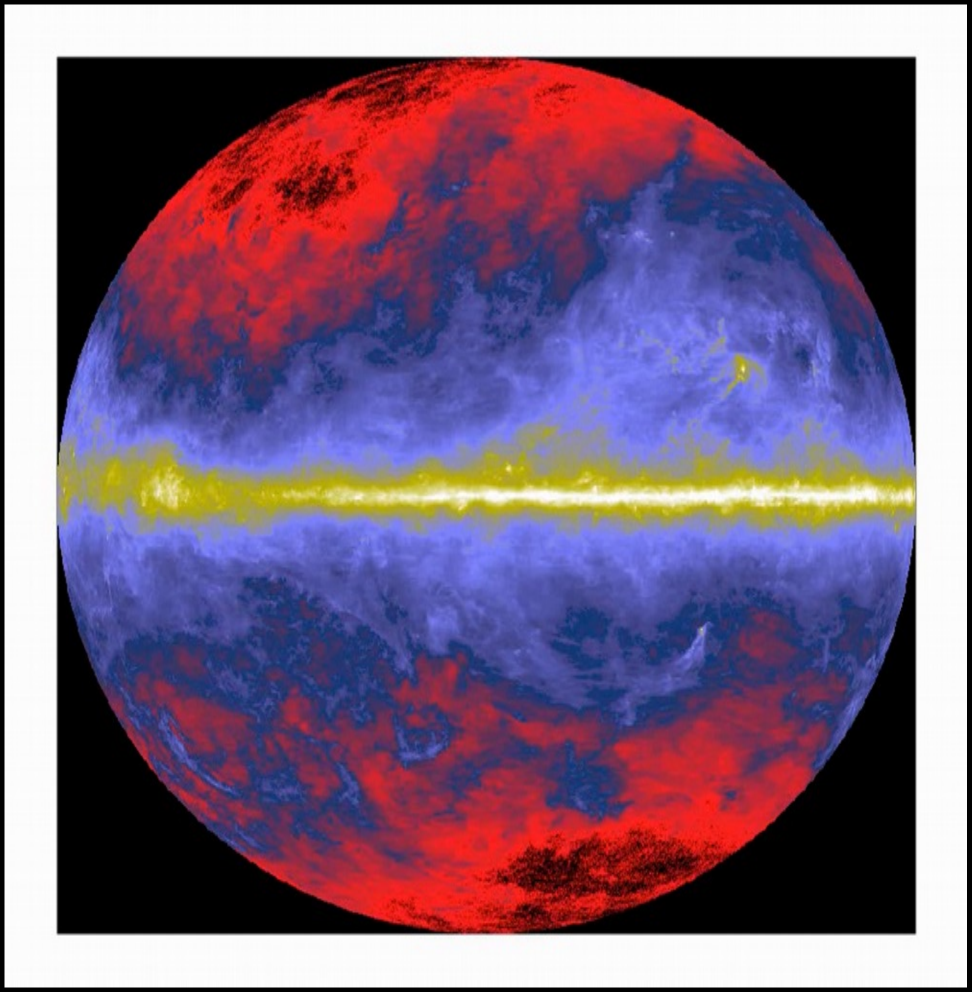

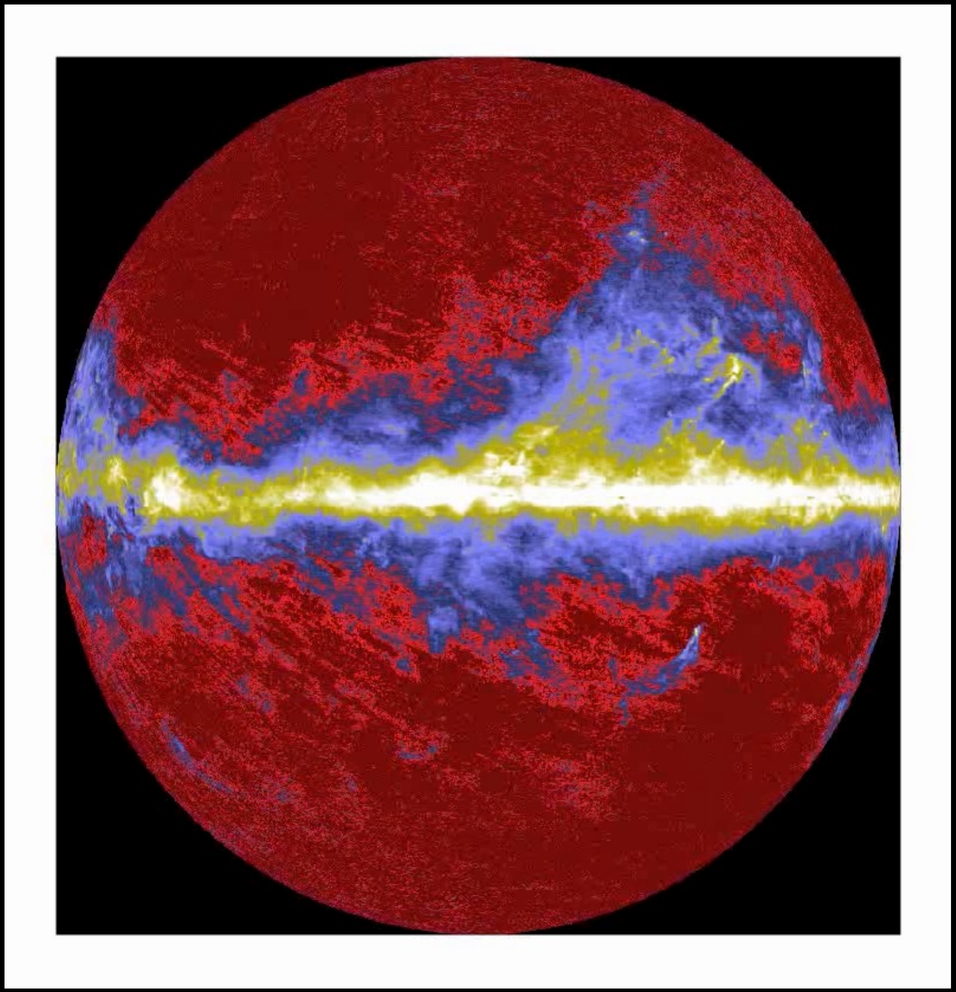

See also Rowles et al. (2009), Dobashi et al. (2011, 2013)

Studies of Galactic Interstellar Clouds and Star Formation

- **Dust emission, scattering, extinction**
  - → structure of filaments, clumps, cores
  - → physical conditions in prestellar clumps
  - → **dust evolution** in star-formation process
  - → role of magnetic fields
- Molecular line studies
  - → formation and stability of cores/clumps
  - → kinematics – accretion and collapse
  - → chemical differences and evolution
- Modelling
  - → interpretation of observations, clump structure, dust evolution, chemistry, B fields, ...